Molecular mechanism of *KIT* and *PDGFRA* mutation and HMGB1 activation in the tumorigenesis of gastrointestinal tumors

Hyun Ju Kang

Department of Medical Science
The Graduate School, Yonsei University

Molecular mechanism of *KIT* and *PDGFRA* mutation and HMGB1 activation in the tumorigenesis of gastrointestinal tumors

Directed by Professor Hoguen Kim

The Doctoral Dissertation
submitted to the Department of Medical Science,
the Graduate School of Yonsei University
in partial fulfillment of the requirements for the degree
of Doctor of Philosophy of Medical Science

Hyun Ju Kang

June 2008

This certifies that the Doctoral Dissertation of Hyun Ju Kang is approved.

Thesis Supervisor: Dr. Hoguen Kim

Thesis Committee Member#1 : Dr. Jeon-Soo Shin

Thesis Committee Member#2 : Dr. Si Young Song

Thesis Committee Member#3 : Dr. Jeon-Han Park

Thesis Committee Member#4 : Dr. Tae Il Kim

The Graduate School

Yonsei University

June 2008

ACKNOWLEDGEMENTS

어린 시절 포메이토에 관한 글을 읽은 그 순간부터 지금까지 저를 계획하시고 이끌어주시며 항상 함께 해 주신 하나님께 감사 드립니다. 긴 시간 동안 연구자로서의 정열과 스승으로서의 혜안으로 지도해 주신 김호근 교수님께 깊은 감사를 드립니다. 논문을 마치기까지 세심한 지도와 조언을 해주신 박전한 교수님, 신전수 교수님, 송시영 교수님, 김태일 교수님께 감사 드립니다. 마이크로 어레이 실험을 가르쳐 주신 남석우 교수님과 프로테오믹스 실험과 원리에 대해 많은 토의를 해주신 안영희 박사님께도 감사 드립니다.

처음 실험실에 와서 아무것도 모를 때 많은 도움을 주신 김남균 선생님, 이용산 선생님, 김현기 선생님, 최연락 선생님 지금 미국에서 열심히 연구를 하고 있을 보고 싶은 고귀혜 선생님, 항상 웃는 표정으로 열심히 연구하는 스마트 권태, 너무 착하고 열심히 해서 다 가르쳐 주고 싶은 귀염둥이 한나, 좀 돌아왔지만 누구보다 힘을 내고 있는 희정이, 미국에서 학위과정을 하고 있는 멋진 희진이와 곧 시작할 귀여운 은기, 동갑내기지만 정말 어른스러운 믿음의 친구 세경이, 밝은 얼굴로 시원시원하게 일을 처리하는 똑순이 세미와 소희 닮은 민지, 지금은 함께 있지 못하지만 항상 마음 써주는 정진 언니, 명진 언니, 승연 언니, 아무 때나 찾아가도 항상 반갑게 맞아주는 마음과 몸의 쉼터 같은 윤희 언니와 호선 언니, 실험적으로 많은 도움을 주신 윤주호 선생님 모두 학위 과정 중에 얻게 된 큰 선물입니다. 항상 바쁜척하던 친구에게 싫은 내색 없이 지켜봐 주고 응원해 주던 16 년 우정 은주, 신혼생활에 빠져있는 하영이, 예쁘고 똑똑한 성이, 결혼하고 더 멋있어지는 혜진이, 피부미인 주영, 착한 과학 선생님 석미, 늙지도 않는 미인 family 민정, 지선, 윤희, 국악의 현대화에 앞장서는 효숙이, 목소리 예쁜 통역관 니나, 노래 잘하는 세민, 용국, 광민, 성훈, 영수, 창하, 멋지게 살고 있는 대학 동기 소라, 수만, 미정, 지원, 글 잘 쓰는 기웅이, 어느덧 10 년 지기가 되어버린 환진 오빠, 경삼 오빠, 동욱 오빠, 호철 오빠, 어쩌다 보니 더 친해진 미소천사 경아 언니와, 공주 보영 언니, 같은 길을 가고 있는 동갑내기 연구원 경아, 곧 엄마가 될 귀여운 정원이, 항상 마음의 친구로 남아 있는 유선이와 지현이 긴 시간 동안 함께 해준 소중한 인연들께도 감사를 드립니다.

지금까지 부족한 저를 세상에서 가장 귀하게 여겨 주시고 항상 격려와 믿음을 보내주신 사랑하는 부모님께 감사 드리며, 딸처럼 아껴 주시는 시부모님과 항상 시원시원한 임선·기선 언니, 옆에서 궂은 말 없이 항상 지켜봐 주고 힘을 주는 든든한 나무 같은 오빠와, 이제는 듬직하게 큰 동생 승현이와 우리 집의 귀염둥이 막내 승권이 에게도 감사의 마음을 전하고 싶습니다.

강현주 올림

Table of contents

LIST OF FIGURES

LIST OF TABLES

ABSTRACT

Molecular mechanism of *KIT* and *PDGFRA* mutation and HMGB1 activation in the tumorigenesis of gastrointestinal tumors

Hyun Ju Kang

Department of Medical Science

The Graduate School, Yonsei University

(Directed by Professor Hoguen Kim)

Activating mutations of *KIT* and *platelet-derived growth factor receptor α (PDGFRA)* are known to be alternative and mutually exclusive genetic events in the development of gastrointestinal stromal tumors (GISTs) through similar pathways; however the specific downstream pathways and their impact on the gene expression profile have not been evaluated. In order to investigate the molecular characteristics of GISTs according to mutation status and genetic features, gene and protein expression profiles in 23 GISTs were analyzed using oligonucleotide microarray containing 18,665 human oligolibrary, and two-dimensional electrophoresis and matrix-associated laser desorption ionization mass spectrophotometry-time of flight, respectively. The mutation status of *KIT* and *PDGFRA* was directly related to the expression levels of activated KIT and PDGFRA, and was also related to the different

expression levels of activated proteins that play key roles in the downstream of the receptor tyrosine kinase III family. To evaluate the impact of mutation status and the importance of the type of mutation in gene expression and clinical features, microarray-derived data from 22 GISTs were interpreted using a principal components analysis (PCA). Three relevant principal components, representing mutation of *KIT*, *PDGFRA* and chromosome 14q deletion were identified from the interpretation of the oligonucleotide microarray data with the PCA. After supervised analysis, there was at least a 2-fold difference in expression between GISTs with *KIT* and *PDGFRA* mutation in 70 genes.

Comparative analysis of the respective spot patterns using two-dimensional electrophoresis showed that 15 proteins were differently expressed the according to mutation status. Expression levels of Septin and Heat shock protein 27 were increased in GISTs with *KIT* mutations, Keratin 10 was overexpressed in GISTs with *PDGFRA* mutations, and Annexin V was overexpressed in GISTs lacking either mutation. When we compared these 15 proteins to tumor grade, 5 proteins (Annexin V, HMGB1, C13orf2, Glutamate dehydrogenase 1, and Fibrinogen beta chain) were overexpressed in malignant GIST relative to benign GIST, while, RoXaN protein levels were lower in malignant GIST. HMGB1 is a non-histone nuclear factor protein that interacts with several transcriptions factors and plays a role in tumor metastasis after secretion. All of the 12 GISTs expressed HMGB1 and especially, malignant GISTs showed more than 2.35 times higher expression level than the benign GISTs.

These findings demonstrate that mutations of *KIT* and *PDGFRA* affect some

different gene and protein expressions, and can be used for the molecular classification and diagnostic biomarker of GISTs. The overexpression of HMGB1 is common in high grade GISTs, and may play a role in the tumorigenesis of GISTs because overexpressed HMGB1 can accelerate genes related to tumor growth and invasion.

Key words: gastrointestinal stromal tumor, KIT, PDGFRA, gene expression profile, oligonucleotide microarray, proteomics, HMGB1

Molecular mechanism of *KIT* and *PDGFRA* mutation and HMGB1 activation in the tumorigenesis of gastrointestinal tumors

Hyun Ju Kang

Department of Medical Science
The Graduate School, Yonsei University

(Directed by Professor Hoguen Kim)

CHAPTER I.
The implication of Receptor Tyrosine Kinase (KIT or PDGFRA) mutations in the tumorigenesis of gastrointestinal stromal tumor

I. INTRODUCTION

In multicellular organism, communications between individual cells are essential for the regulation and coordination of complex cellular processes[1]. Cells respond to external stimuli at the surface of the cell and transduce them to the downstream effecter molecules. This signal transduction process coordinates cellular functions such as cellular growth, differentiation, migration, eruption and extinction, and it occurs through the receptors that are the primary mediators of such physiological cell responses[2, 3]. On the other hand, imbalance of these communication networks

sometimes underlies cause of various diseases such as cancer. For continuous proliferation of cancerous cells, change of signal regulation mechanism should be accompanied.

Receptor Tyrosine Kinases (RTKs) are representative molecules that provoke cell reaction. RTKs can be divided into 20 subfamilies which share a homologous domain that specifies the catalytic tyrosine kinase function, on the basis of their structural characteristics. Deregulations of more than 30 RTKs have been reported to the implicated in human cancer. Alterations of RTKs such as the generation of oncogenic fusion proteins, oncogenic mutations and overexpression had been reported. Some mutations of RTKs cause the receptors to be constitutively activated regardless of outside stimulation and deliver growth signal to downstream molecules[1, 4-6].

Effect of RTKs mutation on the tumorigenesis of gastrointestinal stromal tumor (GIST), the most common mesenchymal tumors of the gastrointestinal tract, has been extensively studied[7-9]. Molecular genetic studies demonstrated that gain-of-function mutations of the *v-kit Hardy-Zuckerman 4 feline sarcoma viral oncogene homolog* (*KIT*) protooncogene, a member of receptor tyrosine kinase III family, are the most frequent and important changes contributing to the development GISTs. Mutations in *KIT* result in ligand independent kinase activity and autophosphorylation of KIT. The *KIT* mutation is known to be present in range from 41 to 92% of GISTs[10-13]. Recently, activating mutations in the *Platelet Derived Growth Factor Receptor α* (*PDGFRA*) gene have been reported in a subset of GISTs lacking *KIT* mutations[14]. *KIT* and *PDGFRA* belong to the same subfamily of receptor tyrosine kinases III[6, 15]. Thus, the

mutually exclusive activating mutations of *KIT* and *PDGFRA* appear to contribute to the development of GIST through similar pathways[16].

Although the activating mutations of *KIT* and *PDGFRA* appear to contribute to the development of GISTs through similar pathways, the specific downstream pathways, and their impacts on the gene expression have not been evaluated. Identification of specific signal pathway can clarify the causes the different biological behavior and drug susceptibility[17, 18].

We therefore performed transcriptional and translational expression studies and compared the results with respect to the different mutation status. We also evaluated the biological significance of one of the activated proteins, HMGB1, and analyzed its role in the tumor progression.

II. MATERIAL AND METHODS

1. Patients and GISTs Tissue Samples

Twenty-three GISTs of the stomach were included in this study. All cases were identified prospectively and consecutively in the Department of Pathology at Yonsei University Medical Center from September 1995 to November 2002 for molecular marker studies. Authorization for the use of those tissues for research was obtained from the Institutional Review Board. Among these 23 GISTs, we used 22 cases for the microarray analysis and we used 12 cases for the proteomics analysis. Information on demographic features and tumor sites was obtained from hospital chart and clinicians. The subjects of study included 13 females and 9 males ranging in age from 36 to 78 years (Table 1). Conventional pathologic parameters (tumor size, number, and grade) were examined prospectively without prior knowledge of the molecular data. The tumor grade of GISTs was divided into three groups according to the criteria of Lewin.

For DNA and RNA extraction, fresh tumors were obtained immediately after surgical excision, and stored at -70°C before use. To enrich the tumor cell population, areas containing more than 90% of tumor cells were sampled from hematoxylin-eosin stained slides using the cryostat microdissection technique. Genomic DNA was prepared using the sodium dodecyl sulfate-proteinase K and phenol-chloroorm extraction method.

Table 1. Clinicopathological and genetic features of 23 GISTs

Array	*Proteomics*	*Loss of*	*Type of Mutation*		*Grade*	*Tumor*	*Sex*	*Age*	*Immunohistochemistry*		
NO.	*No.*	*14q*	*KIT*	*PDGFRA*		*size (cm)*			*KIT*	*PDGFRA*	*CD34*
1		Y	wild	D842V	benign	5	F	47	—	+	+
2	1	Y	W557R	wild	malignant	7	M	52	+	+	+
3	2	Y	wild	D842V	benign	2.5	M	64	—	+	+
4		Y	V560 del	wild	borderline	8	F	76	+	+	+
5		N	V559A	wild	malignant	12	F	56	+	+	+
6		Y	D579 del	wild	borderline	17	F	64	+	+	+
7	3	N	T574 R586 ins	wild	borderline	9	M	45	+	—	+
8	4	Y	wild	wild	borderline	5	F	57	—	+	+
9	6	N	wild	wild	malignant	17	M	78	+	—	+
10	7	N	M552 Y553 del	wild	benign	4	F	39	+	+	+
11	8	Y	V559D	wild	malignant	5.5	F	68	+	+	+
12	9	Y	Y553 Q556 del	wild	malignant	6	M	58	+	+	+
13		Y	W557 G564 del	wild	borderline	10.5	M	53	+	+	+
14		N	V559D	wild	malignant	16	M	58	+	+	+
15		Y	D579 del	wild	benign	4	F	74	+	+	+
16		Y	K550 Q556 del	wild	malignant	8.5	F	67	+	—	+
17	10	N	Q575 R589 ins	wild	borderline	4	F	60	+	+	+
18	11	N	wild	D842V	benign	1.5	M	52	—	+	+
19		N	W557R	wild	malignant	9.8	F	43	+	—	+
20		Y	L556 D569 ins	wild	malignant	33	F	42	+	+	+
21		N	A504 Y505 ins	wild	malignant	6.6	M	65	+	—	—
22	12	Y	V559D	wild	benign	3.5	F	42	+	+	+
	5	NI	wild	D842V	malignant	10	M	35	—	+	+

NOTE. del, deletion; ins, insertion; +, expression; −, no expression; Y, deletion of 14q; N, no deletion

2. Mutation Analysis of *KIT* and *PDGFRA*

Somatic mutations in exons 9, 11, 13 and 17 of *KIT*, and mutations in exons 12 and 18 of *PDGFRA* were analyzed in our 22 GISTs using PCR-based assay as described previously[11, 13, 16, 19, 20]. PCR products were separated on 6% polyacrylamide gels, followed by autoradiography for single strand conformational polymorphism analysis. The PCR products were also sequenced using an ABI Prism 310 Genetic Analyzer (Applied Biosystems, Foster City, CA).

3. Microarray Formulation and RNA Preparation and Hybridization

High-density spotted oligonucleotide microarrays were manufactured at the array core facility at Genome Institute of Singapore. The human OligolibraryTM was purchased from Compugen/Sigma-Genosys. It consisted of 18,861 oligonucleotides, representing 18,664 LEADSTM clusters and 197 controls (GAPDH). Sixtymers of synthesizes oligomers were robotically printed and processed.

Total RNA was extracted from microdissected frozen tissues using an RNeasy Mini kit (Qiagen, Valencia, CA) according to the manufacturer's instructions. 20 ug of total RNA was used as input for cDNA target synthesis as previously described[21]. The targets and Universal Human Reference RNA (Stratagene, La Jolla, CA) were hybridized to an oligonucleotide microarray containing 18,664 probe sets representing 18,664 unique (LEADSTM) genes, and the array was scanned using GenePix scanners. Expression values for each gene were calculated by using the GenPix Pro 4.0 analysis software.

4. Hierarchical Clustering

Unsupervised hierarchical clustering analysis was used to classify the 22 GISTs according to the gene expression. We used a data set of genes that satisfied the filtering criteria: genes having more than 70% of log-transformed ratio values (presenting in across all arrays) were taken and genes with less than 0.35 standard deviations of log-transformed ratio were discarded. The selected gene data set was then applied to complete-linkage hierarchical clustering analysis using the uncentered correlation similarity metric method in Cluster version 2.20. The results of expression map were visualized with Treeview version 1.60 software (http://rana.lbl.gov/EisenSoftware.htm).

5. Principal Component Analysis

Principal component analysis (PCA) is one of the unsupervised approach techniques. In contrast to hierarchical clustering, PCA permits sample classification into multiple independent components. PCA searches for key components in a multidimensional data set to explain differences among the observations[22]. Initially, the set of genes (that had 100% of log-transformed ratio values presenting in all array) were selected. The data of the selected genes was applied to PCA by using Cluster version 2.20. The data of 22 components and eigen values for each component were obtained. We compared each component with clinicopathological data, the status of *KIT* and *PDGFRA* mutation, and deletion of long arm of chromosome 14.

6. Identification of Differentially Expressed Genes According to the Mutation Status of *KIT* and *PDGFRA*

To determine whether GISTs can be classified according to the mutation status of *KIT* or *PDGFRA*, 20 cases (17 with *KIT* mutation and 3 with *PDGFRA* mutation) of GISTs were assessed using the two-way hierarchical clustering analysis. To detect differentially expressed genes according to the mutation status of *KIT* or *PDGFRA*, we ranked the genes using the Mann-Whitney rank sum test. Outlier genes responsible for GISTs with *KIT* or *PDGFRA* mutation were selected by $p < 0.01$. In addition, significant outlier subset genes were further narrowed down by filtering genes showing greater than ± 2 fold expression changes in GISTs with *KIT* mutation compared to the average values from GISTs with *PDGFRA* mutation.

7. Immunoblot and Immunoprecipitation Analysis

Whole lysates from tumor specimens were prepared using lysis buffer [50 mM Tris (pH 7.4), 1 % Triton X-100, 5 mM EDTA, 1 mM KCl, 140 mM NaCl, 2 mM $MgCl_2$, 1 mM phenylmethylsulfonyl fluoride, 1 mM sodium fluoride, 1% aprotinin, 1 μM leupeptin, and 1 mM sodium ortho-vanadate]. 20 g of total protein lysate was loaded into each lane, size-fractionated by SDS-PAGE, and transferred to a Polyvinylidene difluoride membrane that was blocked with Tris-buffered saline-Tween 20 containing 5% nonfat milk. Primary antibodies, KIT (Santacruz Biotech, Santa Cruz, CA), PDGFRA (Santacruz Biotech), glyceraldehyde-3-phosphate dehydrogenase (G3PDH; Trevigen, Gaitherburg, MD), Erk1/2 and phospho-Erk1/2 (Santacruz Biotech), STAT3

and phospho-STAT3 (Cell signaling, Beverly, MA), AKT and phospho-AKT (Cell signaling) and phosphotyrosine-HRP (Amersham Pharmacia Biotech, UK) were incubated for 1 h at room temperature. After washing, membranes were incubated with HRP-conjugated secondary antibody (Santacruz Biotech), washed and then developed with ECL-Plus (Amersham Pharmacia Biotech).

500 μg of tissue lysate was pre-cleared and gently rocked on an orbital shaker with antibodies for immunoprecipitation: anti-KIT (Santa Cruz Biotech) or anti-PDGFRA (Santa Cruz Biotech) at 4°C. The immune complexes were collected by centrifugation and boiled to dissociate the immunocomplexes from the beads. The beads were collected by centrifugation and protein separation was performed by SDS-PAGE with the supernatant fraction.

8. Immunohistochemical Analysis

The tissue array was constructed from formalin-fixed and paraffin-embedded tissues (Petagen Inc., Seoul, Korea) and used for the immunostaining. Deparaffinization and rehydration were performed using xylene and alcohol. The sections were treated with 0.3% hydrogen peroxidase for 3 min and blocking antibody for 30 min. The antibodies used were as follows: KIT [polyclonal, DAKO; 1:1000 (v/v)], PDGFRA [polyclonal, Santacruz Biotech; 1:200 (v/v)], and CD34 [monoclonal, DAKO; 1:50 (v/v)]. The avidin-biotin complex methodology was employed. The chromogen was diaminobenzidine and counterstaining was done with methyl green. The staining of KIT, PDGFRA, and CD34 were categorized as either expressed and absent: cases with

definite staining in more than 10% of the tumor cells were categorized as expressed, and cases with staining in less than 10% of the tumor cells were categorized as absent.

9. 2-Dimensional Electrophoresis (2-DE)

GISTs were suspended in sample buffer containing 40 mM Tris, 7 M urea, 2 M thiourea, 4% CHAPS, 100 mM 1,4-dithioerythritol, and protease inhibitor cocktail (Complete, Roche, Mannheim, Germany). The suspensions were sonicated for approximately 30 s and centrifuged at 100,000 x g for 45 min. 1 mg of total protein from each of 12 GISTs were used for each electrophoresis. Aliquots of proteins in sample buffer were applied to immobilized pH 3 to10 non-linear gradient strips (IPG, immobilized pH-gradient strips, Amersham Pharmacia Biotech, Uppsala, Sweden). Isoelectric focusing (IEF) was conducted at 80,000 Vh. The second dimension was carried out in 9% to16% linear gradient polyacrylamide gels (18 cm x 20 cm x 1.5 mm) at 40 mA per gel at constant current for approximately 5 h, until the dye front reached the bottom of the gel.

10. Protein Visualization and Image Analysis

After protein fixation in 40% methanol and 5% phosphoric acid for 12 h, gels were stained with Coomassie Blue G250 for 24 h. Gels were destained with H_2O and scanned in a Bio-Rad G710 densitometer. The data was converted into electronic files, which were then analyzed using ImageMaster 2D Platinum software (GenBio, Geneva, Switzerland). In order to examine the reliability of the data, only spots showing

greater than ± 2 fold expression changes, compared to the average values from each three classes according to the mutation status, were selected.

11. Protein Spot Identification

For mass spectrometry fingerprinting, protein spots were directly cut out of the gels, destained, and treated with trypsin. Aliquots of the peptide mixtures obtained by trypsin treatment were applied to a target disk and allowed to air-dry. Spectra were obtained using a Voyager DE PRO MALDI-TOF spectrometer (Applied Biosystems, Foster City, CA). Protein database searching was performed with MS-Fit (http://prospector.ucsf.edu/ucsfhtml3.4/msfit.htm) using monoisotopic peaks. A mass tolerance was first allowed within 50 ppm and subsequently reduced to 20 ppm after obtaining the protein lists.

12. Semi-quantitative RT-PCR

Total RNA was isolated using an RNeasy Mini Kit (Qiagen, Valencia, CA), and cDNA synthesis was performed using M-MLV reverse transcriptase (Invitrogen Life Technologies, Rockville, MD, USA), both according to the manufacturer's recommendations. The linear amplification ranges for the genes were examined during serial PCR cycles, and the optimal numbers of PCR cycles were determined. The relative intensity of mRNA expression for each sample was then normalized versus *β-actin* as a surrogate for total mRNA. For each gene, the GenBank accession numbers and the sequences of forward and reverse primers are listed in Table 5. After RT-PCR,

10 μL aliquots of the products were subjected to 2% agarose gel electrophoresis and stained with ethidium bromide.

Table 5. Primers of the 12 genes used for RT-PCR analysis

Gene name	Accession No.	Forward primer (5'-3')	Reverse primer (5'-3')
RoXaN protein	NM_017590	AGCTCTGCTACCCCAAGACA	GCAGAGGAAGGTGAAGATGC
Apolipoprtein A-1 precursor	NM_000039	GGCCGTGCTCTTCCTGAC	GGTTTAGCTGTTTTCCCAAGG
Heat shock protein 27	NM_001540	CTTCACGCGGAAATACACG	CATCGGATTTTGCAGCTTCT
HMGB1	NM_002128	ATATGGCAAAAGCGGACAAG	TGCAGCAATATCCTTTTCGT
Glutathione S-transferase omega 1-1	NM_004832	AGGACGCGTCTAGTCCTGAA	CCAAGGATGGCACCTTAGAA
Annexin V	NM_001154	GGGAGCTGGAACAAATGAAA	CAATTCCAGCATCAGGGTCT
C13orf2	NM_138444	ACAGCACACGTGGATTACCC	ATCCAGGATGTAGCGGAAGA
Aldo-keto reductase family member B1	NM_001628	TGAGTGCCACCCATATCTCA	GGGTAATCCTTGTGGGAGGT
Septin SEPT8_v3	XM_034872	GTCAGCAAGTCGGTCACTCA	TGGGCCTGTAACTCTCATCC
Keratin 10	NM_000421	GAACCACGAGGAGGAAATGA	GCTTCCAGGGATTGTTTCAA
Glutamate dehydrogenase 1	NM_005271	GGGAGGTATCCGTTACAGCA	CCTATGGTGCTGGCATAGGT
Lamin A/C	NM_170708	ACCAAGAAGGAGGGTGACCT	CACGCAGCTCCTCACTGTAG
β-actin	NM_001101	TGTATGCCTCTGGTCGTACCAC	ACAGAGTACTTGCGCTCAGGAG

III. RESULTS

1. Clinicopathologic Characteristics and Mutation Status of *KIT* and *PDGFRA* in GISTs

Among the 23 GISTs, six cases were identified as benign (very low or low risk), six cases as borderline (intermediate risk) and eleven cases as malignant (high risk). Immunoreactivity for KIT was present in 18. Immunoreactivity for CD34 and PDGFRA were found in 22 and 18 cases, respectively. 14q deletion was detected in 13 cases. *KIT* mutation was detected in 17 out of 23 cases. Among the 17 *KIT* mutations, 16 of them were present in exon 11 and one mutation was present in exon 9. Deletion mutations were most frequent and were found in seven cases, while point mutations were found in six cases and insertions in four cases. Among the remaining six cases lacking *KIT* mutations, four cases had *PDGFRA* mutation; all of them were being point mutations in exon 18 (Table 1).

2. Unsupervised Clustering Analysis Distinguish a Subset of GISTs with Lacking *KIT* Mutation

To evaluate the impact of mutation status and the importance of the type of mutation in gene expression and clinical feature performed 19K human oligonucleotide microarray. The relative expression of each gene was evaluated by comparing the degree of the expression to the Universal Human Reference RNA. All of the data of the samples described in this study are presented on our web page (http://www.molpathol.org/data/GIST-arraydata.txt). With a relevant set of 4693 pre-

filtered genes (see “Materials and Methods”), we conducted a complete-linkage hierarchical clustering analysis of 22 arrays. A two-way hierarchical clustering analysis did not completely distinguish GISTs with *KIT* mutation and those lacking *KIT* mutation. However, 13 out of 17 GISTs with *KIT* mutations formed a cluster separated by two small clusters. Moreover, among the 5 GISTs lacking *KIT* mutation, 3 GISTs with *PDGFRA* mutation and 1 GIST lacking both *KIT* and *PDGFRA* mutations formed a cluster (Figure 1).

Next, the data was applied principal component analysis (PCA) that allows classification of 22 samples with multiple components. The correlations between each component and the corresponding genetic and clinical characteristics were analyzed for statistical significance. Component 1 was correlated significantly with the 14q deletion status (P=0.0005, Mann–Whitney rank-sum test, Table 2, Figure 2A), and component 5 and 9 were significantly correlated with the *KIT* and *PDGFRA* mutation status (P=0.01, Mann–Whitney rank-sum test, Table 2, Figure 2B). Three-dimensional scatter plot of values for component 1 (Y axis), component 5 (Z axis) and component 9 (X axis). Red circles indicate GISTs with the loss of chromosome 14q, and blue circles indicate the GISTs without the loss of chromosome 14q. This plot demonstrates that subcategories of GISTs are present according to 14q deletion and *PDGFRA* mutation status. Three GISTs with *PDGFRA* mutation form a separate cluster on the plot (marked by an ellipse).

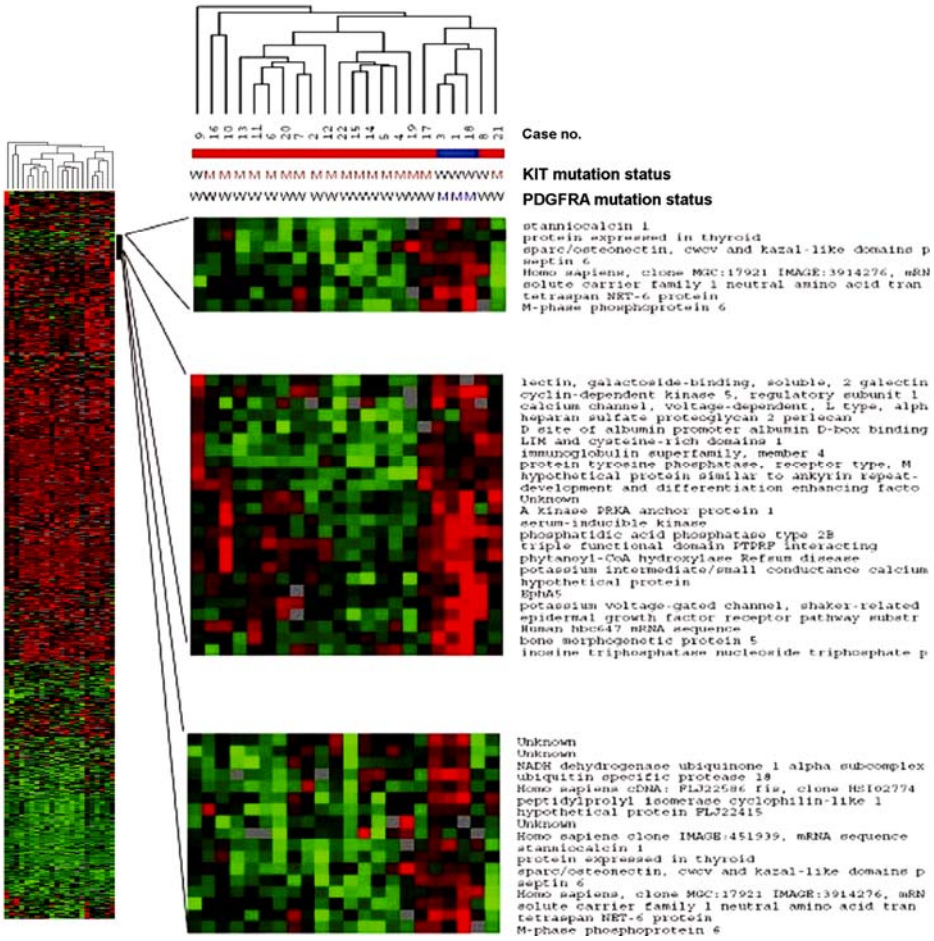

Figure 1. Two-way hierarchical cluster analysis of gene expression patterns, and mutation status of *KIT* and *PDGFRA* (M, mutated type; W, wild type) of 22 GISTs. Genes that passed the cutoff filtering criteria were used (gene expression values present in more than 70% of all arrays were taken, and genes showing standard deviation values of less than 0.35 were discarded). A total of 4,693 genes were selected and applied to complete linkage hierarchical clustering analysis using the uncentered correlation similarity metric method.

Table 2 Correlations between PCA components and tumor characteristics

Categories	Mutation status		Deletion	Tumor Size	Age	Gender	Tumor Cell	Tumor
	PDGFRA	KIT	of 14q	>5	(60>, 60=<)		Type	Grade
Component 1	0.5340	0.8447	0.0005	0.3059	0.7638	0.2167	0.1965	0.3676
Component 2	0.5987	0.6106	0.8674	0.1722	0.4425	0.3006	0.2712	0.2246
Component 3	0.1654	0.8447	0.1330	0.8378	0.2705	0.9734	0.8110	0.8447
Component 4	0.1965	0.8447	0.0101	0.8378	0.5258	0.4425	0.6668	0.7244
Component 5	0.0112	0.0136	0.7134	0.1014	0.6642	0.8674	0.0498	0.1704
Component 6	0.1965	0.0256	0.0663	0.0654	0.5258	0.6642	0.5987	0.2246
Component 7	0.5340	0.0256	0.1511	0.7848	0.7638	0.1018	0.7377	0.3274
Component 8	0.1654	0.7839	0.8674	0.0880	0.8674	0.7134	0.9618	0.0779
Component 9	0.0397	0.7839	0.7638	0.4949	0.5258	0.1018	0.6668	0.5054
Component 10	0.1654	0.1266	0.1330	0.9456	0.2426	0.3673	0.2317	0.1961

NOTE. This table displays the p-values of each correlation between a component (leftmost column) and a tumor characteristic (mutation status, clinical characteristics, top row). Results are shown for the ten components with the highest impact on global molecular phenotype. Mann-Whitney rank sum test were used as statistical tests for characteristics with two subgroups, respectively. For each tumor characteristic, the method of grouping tumors and the number of cases in the relevant group is shown (*Grouping for p-value calculation*; PDGFRA, *PDGFRA*-mutated GISTs; KIT, *KIT*-mutated GISTs; Tumor Cell Type, GISTs with spindle cell type versus GIST with epithelioid and mixed cell type; Tumor Grade, benign GISTs versus borderline and malignant GISTs). Significant those with p-values less than 0.05, are indicated as described in the footnote. Components 1 correlated significantly with loss of chromosome 14q status, while component 5 and 9 correlated significantly with mutation status.

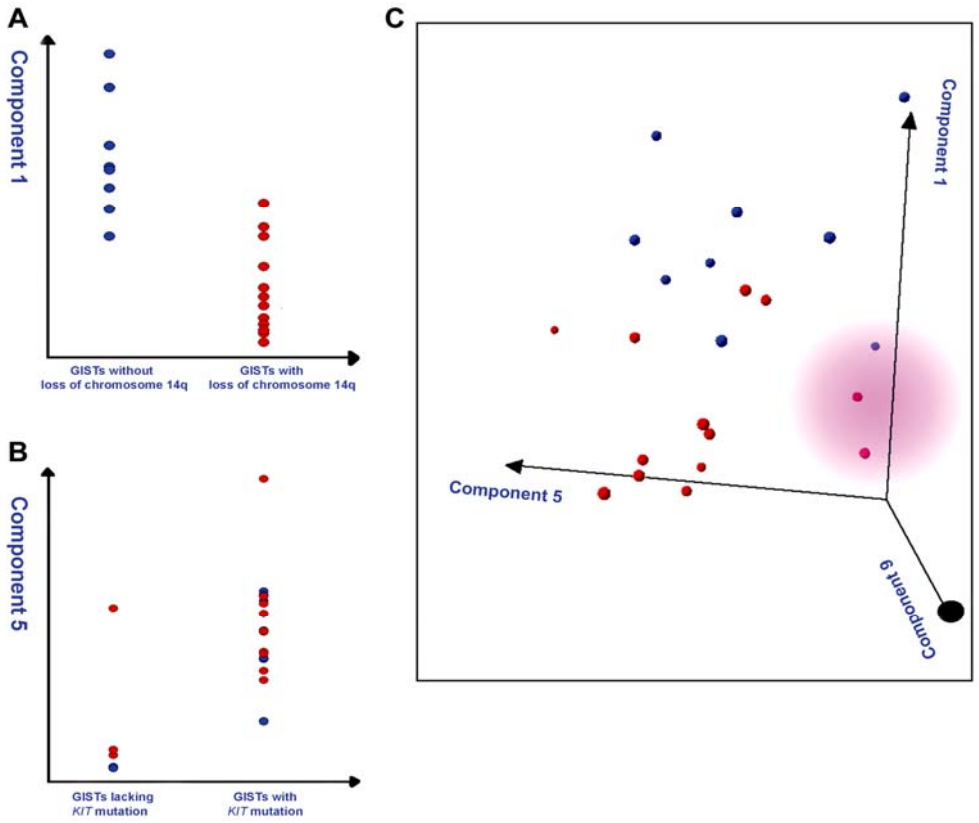

Figure 2. Scatter plots of the output values in component 1, 5. (*A*) one-dimensional scatter plot of component 1 shows that output values for GISTs with 14q deletion were significantly different from those without 14q deletion. (*B*) one-dimensonal scatter plot of component 5 shows that the output values for GISTs with *KIT* mutation were significantly different from the GISTs with *PDGFRA* mutation. (*C*) three-dimensional scatter plot of values for component 1 (Y axis), component 5 (Z axis) and component 9 (X axis). Red circles indicate GISTs with the loss of chromosome 14q, and blue circles indicate the GISTs without the loss of chromosome 14q. This plot demonstrates that subcategories of GISTs are present according to 14q deletion and *PDGFRA* mutation status.

We then tried to identify a robust set of mutation type-related genes by a

supervised rank-sum analysis using the Mann-Whitney rank sum test. To identify the genes that were differentially regulated in GISTs according to the mutation status of *KIT* or *PDGFRA*, we selected 20 GISTs (17 GISTs with *KIT* mutation and 3 GISTs with *PDGFRA* mutation; 2 GISTs lacking both mutations were excluded), and we used a stringent selection criterion (See "Material and Methods"). 70 genes were found to be either up-regulated (7 genes) or down-regulated (63 genes) in 17 GISTs with *KIT* mutation compared to the 3 GISTs with *PDGFRA* mutation. The genes that were differentially expressed in GISTs with *PDGFRA* mutation are listed in Figure 3A and Table 3.

3. Mutation of *KIT* and *PDGFRA* Are Directly Correlated to the Overexpression of Active KIT and PDGFRA

The effect of mutation on the activation of KIT and PDGFRA was examined at the RNA and protein levels (Figure. 3A and 3B). The levels of KIT and PDGFRA protein and their phosphorylation status were analyzed by Western blotting. KIT expression was increased in GISTs with *KIT* mutation (Figure 3B). The average relative expression ratio of KIT was 5.6 in 17 cases with *KIT* mutation and 0.1 in 5 GISTs lacking *KIT* mutation. In contrast, PDGFRA expression was found in GISTs regardless of *PDGFRA* mutation status: 14 out of 17 GISTs with *KIT* mutation expressed PDGFRA in addition to all 3 GISTs with *PDGFRA* mutation. To determine whether KIT and PDGFRA expressions were related to their active forms, we examined their phosphorylation status. Out of 17 GISTs expressing KIT, 14 GISTs

expressed phospho-KIT, whereas phospho-PDGFRA was detected in only 4 out of 17 GISTs expressing PDGFRA (Figure 3B). These results indicate that activation of KIT and PDGFRA was related to the mutation status of *KIT* and *PDGFRA*, respectively, because 13 of 17 GISTs with *KIT* mutation expressed activated KIT and all 3 GISTs with *PDGFRA* mutation expressed activated PDGFRA.

Immunohistochemically, KIT and PDGFRA were detected mainly in the cytoplasm of the tumor cells. KIT expression was detected in 17 GISTs with *KIT* mutation and 1 of 5 GISTs lacking *KIT* mutation. The cytoplasmic PDGFRA expression was detected in all 3 *PDGFRA*-mutated GISTs, 13 of 17 *KIT*-mutated GISTs, and 1 of 2 GISTs lacking both *KIT* and *PDGFRA* mutations (Table 1 and Figure 3C).

4. Expression of Activated STAT3, AKT and Erk1/2 in GISTs with *KIT* and *PDGFRA* Mutation

Since the mutation status of *KIT* and *PDGFRA* was directly related to the expression of activated KIT and PDGFRA, signaling molecules that are known to play key roles downstream of receptor tyrosine kinase III were evaluated in 8 GISTs. STAT3 was analyzed for the evaluation of JAK/STAT pathway, Erk1/2 for the MAPK pathway and AKT for the PI3K pathway. As expected, all of the above molecules were expressed in their active forms in all of 8 GISTs; however, the expression level was different according to mutation status of *KIT* and *PDGFRA*. The expressions of phospho-STAT3 and phospho-AKT were more intense in GISTs with *KIT* mutation

than in those with *PDGFRA* mutation, while expression of phospho-Erk1/2 was stronger in GISTs with *PDGFRA* mutation. There was no difference in the protein expression level of STAT3, AKT and Erk1/2 between our GISTs with *KIT* and *PDGFRA* mutation.

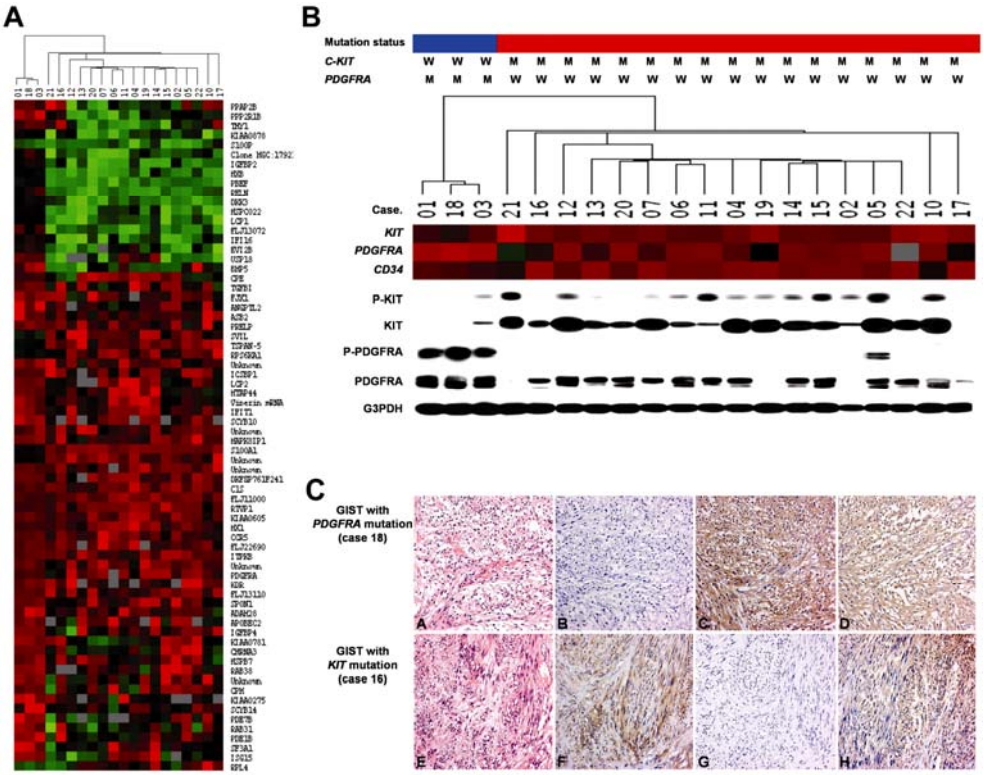

Figure 3. Expression of KIT and PDGFRA at the RNA (*A*) and protein levels (*B* and *C*). (*A*) Supervised hierarchical cluster analysis of gene expression patterns, and the mutation status of *KIT* and *PDGFRA* of 20 GISTs. To detect differentially expressed genes in a given sub-class, we ranked the genes using the Mann-Whitney rank sum test. Outlier genes responsible for mutation status were selected by $p < 0.01$. In addition, significant outlier subset genes were further narrowed by filtering genes showing greater than ±2 fold expression changes in *KIT*-mutated GISTs compared to the average values from *PDGFRA*-mutated GISTs. Cases 1, 3 and

18 showed *PDGFRA* mutation (marked as blue), and the other 17 cases showed *KIT* mutation (marked red). (*B*) RNA expressions of KIT and PDGFRA were correlated to the mutation status of *KIT* and *PDGFRA* (M, mutated type; W, wild type). In contrast, homogenous CD34 expression was noted regardless of *KIT* or *PDGFRA* mutation. 17 GISTs with *KIT* mutation showed an overexpression of KIT and activated KIT protein, while only one (case 3) of 3 GISTs (cases 1, 3, and 8) with *PDGFRA* mutation expressed KIT and showed activated KIT protein. PDGFRA was expressed in 14 of 17 *KIT*-mutated GISTs and all 3 with *PDGFRA*-mutated GISTs; however only one (case 5) out of 17 *KIT*-mutated GISTs and all 3 *PDGFRA*-mutated GISTs (cases 1, 3 and 18) demonstrated activated PDGFRA. (*C*) Example of histological (A and E), and immunohistochemical analysis of KIT (B and F), PDGFRA (C and G), and CD34 (D and F). Overexpression of KIT and PDGFRA was directly correlated to the mutation status of *KIT* and *PDGFRA*, respectively.

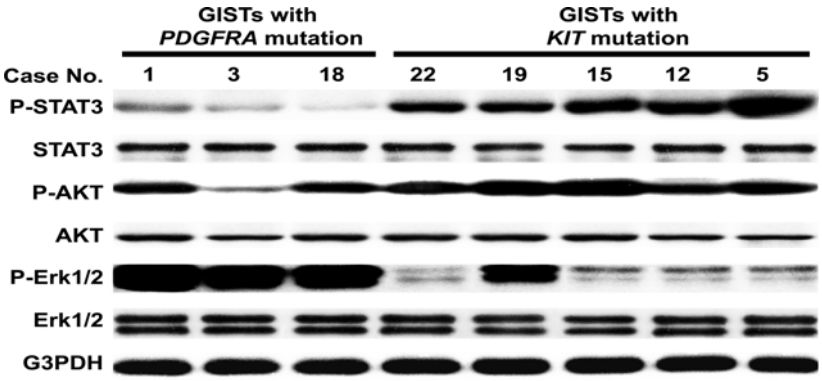

Figure 4. Expression level of activated STAT3, AKT and Erk1/2. Expressions of phospho-STAT3 and phospho-AKT were more intense in GISTs with *KIT* mutation than in those with *PDGFRA* mutation while expression of phospho-Erk1/2 was stronger in GISTs with *PDGFRA* mutation. No difference in the protein expression level of STAT3, AKT and Erk1/2 was noted between 5 GISTs with *KIT* mutation and 3 GISTs with *PDGFRA* mutation.

Table 3. List of ~~genes most~~ differentially expressed known genes ~~between~~ between GISTs with *KIT* mutation and *PDGFRA* mutation

UniGene ID	Gene name	Symbol	GISTs with KIT mutation*	GISTs with PDGFRA mutation†	p value
signal transduction					
Hs.162	insulin-like growth factor binding protein 2	IGFBP2	0.28	2.10	0.007
Hs.2962	S100 calcium binding protein P	S100P	0.48	0.19	0.007
Hs.283016	phosphodiesterase 7B	PDE7B	1.03	2.29	0.008
Hs.89605	cholinergic receptor, nicotinic, alpha polypeptide 3	CHRNA3	1.23	3.80	0.007
Hs.203238	phosphodiesterase 1B, calmodulin-dependent	PDE1B	1.23	8.14	0.007
Hs.2488	lymphocyte cytosolic protein 2	LCP2	1.30	2.63	0.008
Hs.1516	insulin-like growth factor binding protein 4	IGFBP4	1.45	6.06	0.007
Hs.234249	mitogen-activated protein kinase 8 interacting protein 1	MAPK8IP1	1.47	3.99	0.007
Hs.182416	ankyrin repeat and SOCS box-containing 2	ASB2	1.68	13.89	0.007
Hs.12337	kinase insert domain receptor	KDR	1.81	4.50	0.009
Hs.149957	ribosomal protein S6 kinase, 90kD, polypeptide 1	RPS6KA1	1.83	0.81	0.007
Hs.78877	inositol 1,4,5-trisphosphate 3-kinase B	ITPKB	2.22	7.12	0.007
Hs.74615	platelet-derived growth factor receptor, alpha	PDGFRA	4.46	22.39	0.007
Hs.76391	interferon-inducible protein p78 (mouse)	MX1	5.01	19.35	0.007
Hs.292707	S100 calcium binding protein A1	S100A1	12.44	3.20	0.007
development					
Hs.12246	reelin	RELN	0.32	2.58	0.007
Hs.8025	angiopoietin-like 2	ANGPTL2	1.24	5.41	0.007
Hs.200594	KIAA0605 gene product	KIAA0605	3.01	14.30	0.007
protein metabolism					
Hs.38260	ubiquitin specific protease 18	USP18	0.79	2.41	0.008
Hs.833	interferon-stimulated protein, 15 kDa	ISG15	1.07	14.33	0.007
Hs.334691	splicing factor 3a, subunit 1, 120kD	SF3A1	1.08	2.56	0.007
Hs.334873	carboxypeptidase M	CPM	1.30	2.83	0.007
Hs.105468	hypothetical protein FLJ22690	FLJ22690	2.10	5.81	0.008
Hs.169756	complement component 1, s subcomponent	C1S	3.41	12.28	0.007
	cell adhesion				
Hs.289114	hexabrachion (tenascin C, cytotactin)	HXB	0.15	1.12	< 0.01
Hs.74583	KIAA0275 gene product	KIAA0275	1.13	3.59	0.009
Hs.20709	tetraspan 5	TSPAN-5	1.99	0.92	< 0.01
Hs.5378	spondin 1, (f-spondin) extracellular matrix protein	SPON1	3.11	40.85	< 0.01
response to biotic stimulus					
Hs.24395	small inducible cytokine subfamily B member 14	SCYB14	1.11	3.95	< 0.01
Hs.2248	small inducible cytokine subfamily B member 10	SCYB10	1.77	9.83	0.009
Hs.20315	interferon-induced protein with tetratricopeptide repeats 1	IFIT1	1.82	8.87	0.007
nucleobase, nucleoside, nucleotide and nucleic acid metabolism					

Hs.155530	interferon, gamma-inducible protein 16	IFI16	0.54	1.55	0.007
Hs.227457	apolipoprotein B mRNA editing enzyme,2	APOBEC2	1.60	5.83	0.008
Hs.14453	interferon consensus sequence binding protein 1	ICSBP1	1.84	4.34	0.007
cell organization and biogenesis					
Hs.76494	proline arginine-rich end leucine-rich repeat protein	PRELP	1.68	5.95	0.007
Hs.76506	lymphocyte cytosolic protein 1 (L-plastin)	LCP1	0.38	1.09	0.007
Hs.10432	KIAA0878 protein	KIAA0878	0.47	1.20	< 0.01
phosphorus metabolism					
Hs.108705	protein phosphatase 2 A PR 65, beta isoform	PPP2R1B	0.84	3.90	0.007
Hs.42676	KIAA0781 protein	KIAA0781	1.11	2.23	0.007
transport					
Hs.223025	RAB31, member RAS oncogene family	RAB31	0.99	2.38	0.007
Hs.108923	RAB38, member RAS oncogene family	RAB38	1.27	3.44	0.008
others					
Hs.125359	Thy-1 cell surface antigen	THY1	0.68	6.82	< 0.01
Hs.277014	hypothetical gene FLJ13072	FLJ13072	0.73	1.54	0.007
Hs.39384	four jointed box 1 (Drosophila)	FJX1	1.51	5.60	0.007
Hs.239138	pre-B-cell colony-enhancing factor	PBEF	0.37	0.77	0.007
Hs.4909	dickkopf homolog 3 (Xenopus laevis)	DKK3	0.44	1.04	< 0.01
Hs.1104	bone morphogenetic protein 5	BMP5	0.88	2.96	< 0.01
Hs.118787	transforming growth factor, beta-induced, 68kD	TGFBI	1.84	13.47	0.007
Hs.75360	carboxypeptidase E	CPE	2.47	12.52	< 0.01
Hs.64639	glioma pathogenesis-related protein	RTVP1	3.74	9.84	< 0.01
Hs.7358	hypothetical protein FLJ13110	FLJ13110	2.28	8.18	0.007
Hs.173717	phosphatidic acid phosphatase type 2B	PPAP2B	0.98	2.80	< 0.01
Hs.174030	a disintegrin and metalloproteinase domain 28	ADAM28	1.40	6.79	0.007
Hs.54443	chemokine (C-C motif) receptor 5	CCR5	1.52	3.07	< 0.01
Hs.56874	heat shock 27kD protein family, member 7	HSPB7	1.29	2.92	0.007
Hs.154567	supervillin	SVIL	1.86	0.63	0.007

NOTE. *, average of 17 *KIT*-mutated GISTs / Universal Human Reference RNA; †, average of 3 *PDGFRA*-mutated GISTs / Universal Human Reference RNA.

5. Identification of Differentially Expressed Proteins According to Mutation Status and Tumor Progression

These findings suggest that there may be some quantitative differences in the activation of proteins downstream of type III receptor tyrosine kinase between GIST with *KIT* mutations and those with *PDGFRA* mutations, and that these differences may be associated with differential protein expression. To identify the differentially expressed genes according to the type of activating mutation, the protein expression levels in the 12 GISTs were analyzed using 2-DE. (Figure 5A). The 12 GISTs were divided into 3 classes according to their mutation status (8 GISTs with *KIT* mutation, 2 GISTs with *PDGFRA* mutation and 2 GISTs lacking both mutations; Table 1). The analysis of protein expression levels from all samples revealed that 15 proteins were significantly up- or down-regulated in specific classes. The selected spots showed greater than ± 2 fold expression changes compared to the average values from each of the three classes. Of the 15 proteins, nine were up-regulated in the GISTs with *KIT* mutations, three were up-regulated in GISTs with *PDGFRA* mutations, and three were up-regulated in GISTs lacking mutations. Data for these proteins and is shown in Figure 5B and 5C.

When we compared these 15 proteins to tumor grade, 5 proteins (Annexin V, HMGB1, C13orf2, Glutamate dehydrogenase 1, and Fibrinogen beta chain) were overexpressed in malignant GISTs relative to benign GISTs; meanwhile, RoXaN protein levels were lower in malignant GISTs and listed in Table 4.

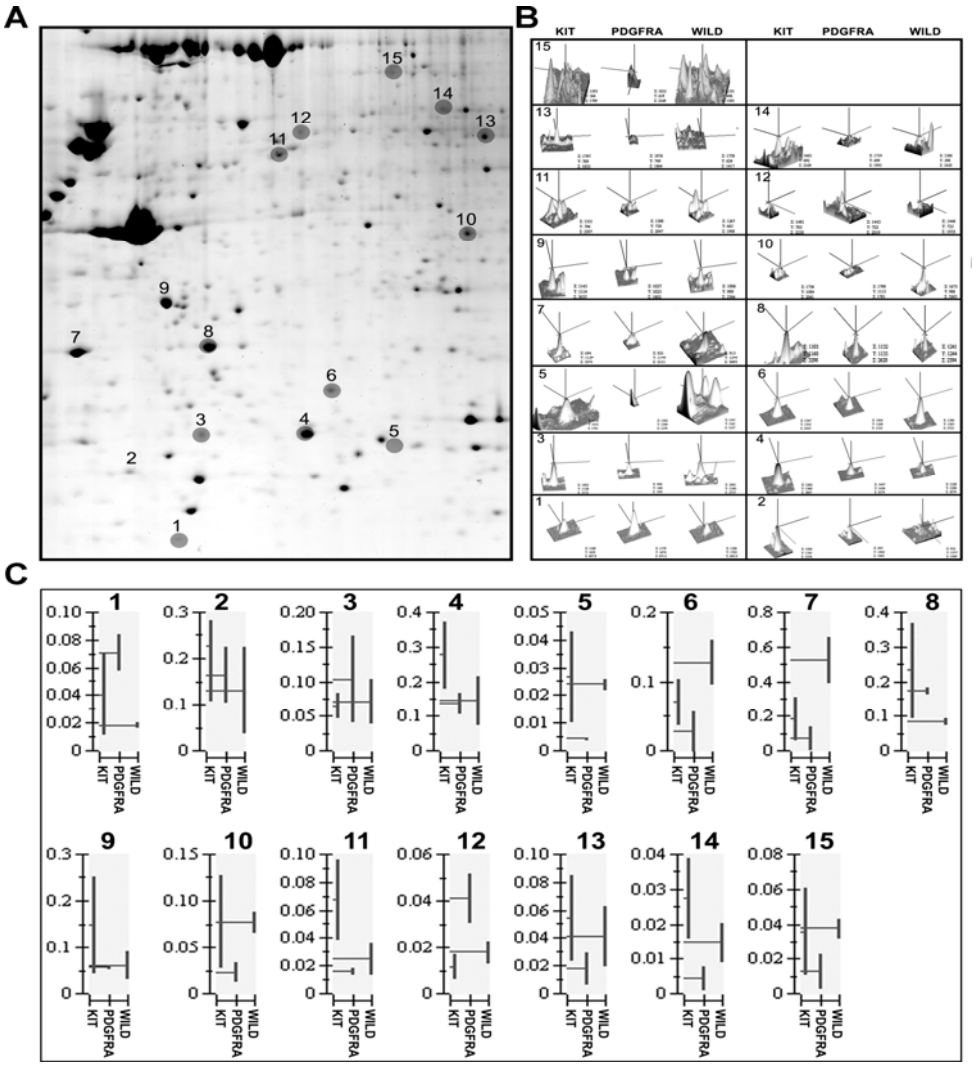

Figure 5. (*A*) Representative two-dimensional electrophoresis (2DE) of a GIST (case 1). The proteins from GISTs were extracted and separated as described in the methods section. The gel was stained with Coomassie blue G250, and protein spots were examined by MALDI-TOF. The circles indicate the location of the proteins. (*B*) 3-Dimesional gel images of 15 proteins. (*C*) Histograms of 15 differentially expressed proteins classified according to tumor mutation status.

Table 4. Correlation between tumor grade and 15 differentially expressed proteins

Group of protein	Protein No	Protein Name	matching peptides No.	% Coverage	Accession No.	Comparative ratio of expression		
						Benign	Borderline	Malignant
Group[a)]	1	RoXaN protein	7	16	34783369	3.33	1.90	1.00
Group[b)]	7	Annexin V	14	37	999937	1.00	2.49	2.01
	5	HMGB1	8	37	123369	1.00	1.64	2.35
	9	C13orf2	12	38	33341268	1.00	2.18	2.89
	13	Glutamate dehydrogenase 1	20	38	4885281	1.00	2.14	2.23
	14	Fibrinogen beta chain	15	32	11761630	1.00	1.91	2.03
Group[c)]	2	Apolipoprtein A-1 precursor	20	54	4557320	1.03	1.43	1.00
	3	NADH dehydrogenase	13	42	5138999	1.44	1.53	1.00
	4	Heat shock protein 27	7	34	662841	1.00	1.58	1.23
	6	Glutathione S-transferase omega 1-1	10	31	55925946	1.00	0.98	1.23
	8	Annexin Family Mol-id	18	57	1421662	1.00	1.54	1.58
	10	Aldo-keto reductase family member B1	13	45	4502049	1.13	1.24	1.00
	11	Septin SEPT8_v3	14	31	27448554	1.95	2.12	1.00
	12	Keratin 10	12	32	40354192	2.51	1.00	1.33
	15	Lamin A/C	13	24	27436947	1.00	2.40	1.35

Group[a)] decreased expression in malignant GISTs

Group[b)] overexpressed in malignant GISTs

Group[c)] no changes in expression between benign and malignant GISTs

6. Verification of Differentially Expressed Proteins by Semi-quantitative RT-PCR

To examine whether the change of differentially expressed proteins was due to transcriptional or other regulatory mechanisms, we examined the mRNA levels of 12 genes by semi-quantitative RT-PCR. The other 3 genes (*Hypothetical protein, Annexin Family Mol-id, Fibrinogen beta chain*) were not included this study, due to failure of

adequate primer design. These were direct correlations between the expression level of mRNA and protein in all of 7 genes overexpressed in GISTs with *KIT* mutation, and 2 genes overexpressed in GISTs with *PDGFRA* mutation, and 3 genes overexpressed in GISTs lacking both mutations.

7. Identification of HMGB1 as a Tumor Marker of GISTs.

We focused on the expression of HMGB1, because some of the reported functions of HMGB1 are related to tumor growth and metastasis. Both the *p*I and the relative molecular mass of HMGB1 in each 2DE gel were determined by comparison with standard 2DE gels from the Swiss-2D-PAGE database. Because we could not find normal matched tissue in GISTs, we compared HMGB1 expression of the GISTs to the 13 colorectal carcinomas and matched normal mucosae. The expression of HMGB1 in colorectal carcinomas and matched normal mucosae was ubiquitous, however marked variations were found. Of the 13 colorectal carcinomas, all tumors and matched normal mucosae showed detectable HMGB1 expression, and 7 tumors showed more than 3 times higher intensity than the matched normal mucosae. Comparison of HMGB1 expression by volume percentage showed higher level expression in colorectal carcinomas and GISTs than the non-tumorous colon mucosae; the average volume percentage was 0.23 ±0.19 for GISTs, 0.31 ± 0.14 for colorectal carcinomas and 0.08 ± 0.06 for non-tumorous colon mucosae (Figure 6). To further examine the molecular characteristics of HMGB1, the HMBG1 spot in 2DE was isolated and subjected to trypsin digestion followed by MALDI-TOF analysis.

HMGB1 was validated by mass fingerprinting of the selected peaks of peptides by applying low tolerance (<20 ppm) with recalibration (Figure 7). For HMGB1, a total of 6 peaks were detected with 37% coverage (Table 6).

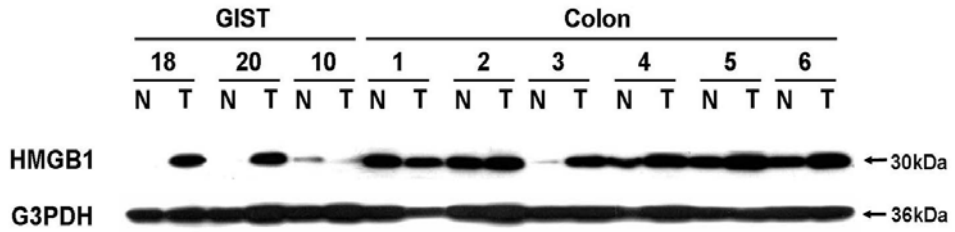

Figure 6. HMGB1 is overexpressed in GISTs and Colon cancer.

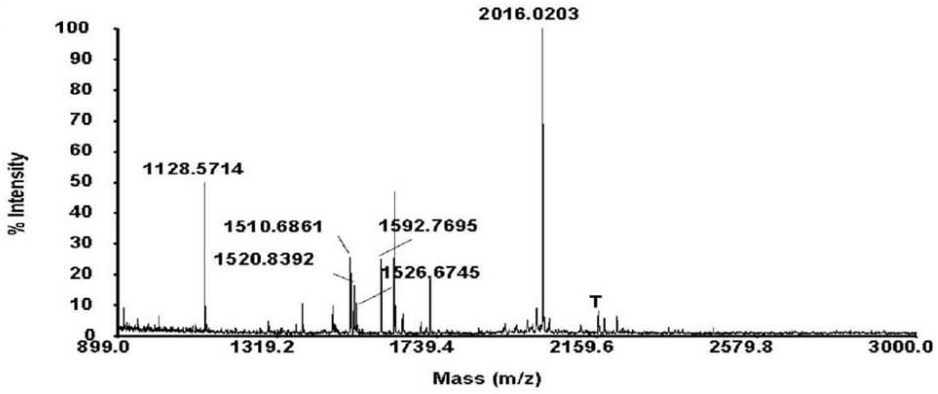

Figure 7. MALDI-TOF peptide mass spectrum of the tryptic digest of HMGB1. T, trypsin autolytic fragments.

Table 6. Summary of MALDI-MS masses obtained from tryptic digests of human HMGB1

Masses Submitted	Monoprotonated Masses, MH+ matched	Delta PPM	Start	End	Proposed Peptide Sequence
1128.5714	1128.5689	2.1	155	163	(K) YEKDIAAYR(A)
1510.6861	1510.6823	2.5	13	24	(K) MSSYAFFVQTCR(E)
1520.8392	1520.8437	-2.9	113	127	(K) IKGEHPGLSIGDVAK(K)
1526.6745	1526.6772	-1.7	13	24	(K) MSSYAFFVQTCR(E)
1592.7695	1592.7709	-0.9	30	43	(K) KHPDASVNFSEFSK(K)
1592.7695	1592.7709	-0.9	31	44	(K) HPDASVNFSEFSKK(C)
1592.7695	1592.7379	19.9	128	141	(K) KLGEMWNNTAADDK(Q)
2016.0203	2016.0166	1.8	97	112	(K) RPPSAFFLFCSEYRPK(I)

Note. A total of 37% of sequence coverage.

Abbreviation: PPM, parts per million.

8. Cytoplasmic Distribution of HMGB1 in GISTs

The nuclear and cytoplasmic expression of HMGB1 was separately measured in 5 GISTs by using fractionated nuclear and cytoplasmic protein lysates. 4 out of 5 GISTs showed variable amount of HMGB1 expression in the nuclear and cytoplasmic proteins, whereas weak or undetectable cytoplasmic expression was found in 1 GISTs, Immunohistochemically, HMGB1 was detected mainly in the nuclei of the tumor cells, cytoplasm of some tumor cells, and some nuclei of the normal cells. In 14 out of 20 GISTs showed nuclear HMGB1 expression and 5 showed cytoplasmic HMGB1 expressions. In the colorectal carcinomas, stronger HMGB1 expression compared to that of the normal mucosal cells was found in most of the tumor cells, however the

level of expression between tumors was variable (Figure 8).

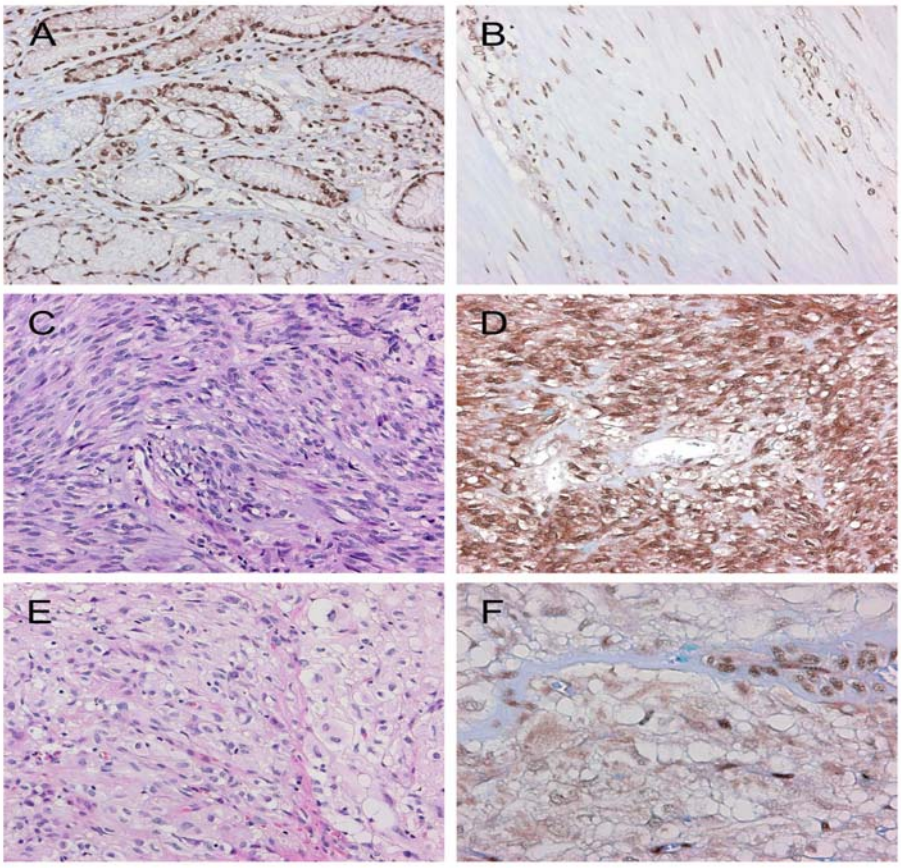

Figure 8. Immunohistochemical analysis of HMGB1 in GISTs. Expression of HMGB1 is noted in the nuclei of epithelial cells and inflammatory cells in the gastric mucosa (*A*) and in the nuclei of smooth muscle cells (*B*). Microscopic feature of a GIST with *KIT* mutation (*C*), which shows strong nuclear and cytoplasmic HMGB1 expression (*D*). Histology of a GIST without *KIT* mutation (*E*) showing no HMGB1 expression in tumor cells. HMGB1 expression is only evident in the nuclei of the vascular smooth muscle cells and capillary endothelial cells (*F*).

IV. DISCUSSION

Mutation of *KIT* has been implicated as a major genetic event in the tumorigenesis of GISTs, because most GISTs have shown gain of function mutation of *KIT* and germline mutation of *KIT* has been found in familial GISTs[23-25]. Recently, the mutation of *PDGFRA* has been considered as another causative genetic event[26, 27] , as *PDGFRA* mutations were found in most of the GISTs lacking *KIT* mutation, and both PDGFRA and KIT belong to the same subfamily of receptor tyrosine kinase III[28, 29]. Thus, it has been speculated that the mutations of these two genes facilitate the transformation and progression of GISTs through the same pathway. We confirmed here that the mutations of *KIT* and *PDGFRA* are mutually exclusive in our GISTs. Furthermore, our data demonstrated that the mutations of *KIT* and *PDGFRA* correlated with protein overexpression and activation. These findings indicate that the mutation of *PDGFRA* directly correlates with the activation of PDGFRA, and may be involved in the tumorigenesis of GISTs.

GISTs show unique chromosomal, morphological and immunohistochemical characteristics. Recently, there have been two studies on the gene expression of GIST, and both have demonstrated that the gene expression profile of GISTs is different from those of the other types of mesenchymal tumors[30 31]. Although these data indicated that GISTs are unique and homogeneous tumors, they show some diverse intertumoral variations at the clinical, morphological and genetic level. Clinically, GISTs are classified as benign, borderline or malignant tumors. Histopathologically, they exhibit two distinct forms, spindle and epithelioid, and mixed patterns are detected in some

cases. In addition, several peculiar histologic patterns, such as alveolar pattern, have been detected in some GISTs. The genetic characteristics of GISTs are also diverse. The loss of the long arm of chromosome 14 was detected in 69 to 80% of GISTs[32 33], and *KIT* mutation was found in 41 to 92% of GISTs[23-25]. In this study, we attempted to classify GIST at the molecular level according to the overall gene expression profiles. Our data suggest that GISTs may be categorized into subsets according to the mutation status of *KIT* and *PDGFRA*. The direct link between molecular classification and the activating mutations should be regarded as an important finding. Different gene expression patterns of the GISTs according to the anatomic tumor site and the different gene mutation status have recently been reported[34]. When we correlated the molecular classification with the clinical, pathological and genetic characteristics by the PCA model, 14q deletion, *KIT* mutation, and *PDGFRA* mutation had the strong impacts. Furthermore, our data revealed that 70 genes are expressed differentially between the *KIT*-mutated GISTs and *PDGFRA*-mutated GISTs. Most of these genes are overexpressed in *PDGFRA*-mutated GISTs. Some of these genes have known functions in signal transduction (ASB2, IGFBP2, IGFBP4, PDGFRA, RPS6KA1, and S100A1) and development (RELN and ANGPTL2). Further analysis in a larger series of cases, and determination of the possible functional mechanism of these differentially expressed genes should clarify the molecular characteristics of *KIT* and *PDGFRA* mutation.

Receptor tyrosine kinase III family that are known to transduce their signals through the JAK/STAT pathway[35, 36 37], Ras/ERK pathway [38], PLC-γ pathway[39, 40],

PI3K pathway[41] and PDK and AKT[42] pathways. All of these pathways have been suggested to contribute to tumor development, as they have been shown to regulate the cell cycle and cell differentiation through the activation of transcription factors[43]. Our oligonucleotide microarray analysis allowed us to evaluate 15 genes (AKT, GRB, JAK, MAP2K, MAPK, PDK, PI3K, PIP3, RAF, RAS, SHC, SRC, STAT1, STAT3, STAT5) that are known to be involved in these signal transduction pathways. There were no remarkable differences in their RNA expression levels in our GISTs with *KIT* mutation and *PDGFRA* mutation. However, we found remarkable differences in the expression levels of activated proteins related to the JAK/STAT, PI3K and MAPK signaling pathways between the *KIT*-mutated GISTs and *PDGFRA*-mutated GISTs. The expressions of phospho-STAT3 and phospho-AKT were more intense in the *KIT*-mutated GISTs than *PDGFRA*-mutated GISTs while expression of phospho-Erk1/2 was stronger in *PDGFRA*-mutated GISTs. These findings suggest that there are some quantitative differences in the activation of the proteins downstream of receptor tyrosine kinase III between *KIT*-mutated GISTs and *PDGFRA*-mutated GISTs, and that these differences may be associated with differential gene expression.

We have analyzed some of the differently expressed genes using oligonucleotide arrays. Moreover, we also demonstrated that mutations in *KIT* and *PDGFRA* were correlated with the different expression levels of activated proteins in the JAK/STAT, PI3K and MAPK signaling pathways. These findings suggest that there are some quantitative differences in the activation of the proteins downstream of receptor tyrosine kinase III between *KIT*-mutated GISTs and *PDGFRA*-mutated GISTs, and

these differences may be associated with differential protein expression.

Using a comparative analysis of the respective spot patterns on two-dimensional electrophoresis, we identified 15 proteins that were differently expressed according to the mutation status of the tumors. Among the15 proteins, the expression levels of Septin and Heat shock protein 27 were increased in *KIT*-mutated GISTs. Among these identified 15 proteins, Heat shock proteins (HSPs) are thought to be molecular chaperones and are known to be essential for the survival of cancer cells by modulating the activity of different proteins involved in cell cycle and apoptosis[44-46]. Overexpression of HSPs is reported to prevent the apoptosis induced by anticancer drugs[47]. The overexpression of HSPs has also been reported in leukemia as well as breast, renal, and bladder cancers[45]. Recently, it has been reported that the serine/threonine kinase AKT directly phosphorylates HSP27 on Ser-82 in vitro and in intact cells[48]. This interaction between HSP27 and AKT may have an important role in cellular function. These reports are in concordance with our previous report that activated AKT was more highly expressed in the GISTs with *KIT* mutations than in those with *PDGFRA* mutations. From these results, we suspect that the constitutive activity of AKT caused by a *KIT* mutation would be related to HSP27 overexpression in *KIT*-mutated GISTs.

We demonstrated the overexpression of HMGB1 in high grade GISTs and the tumor cells are the origin of overexpressed HMGB1 by immunohistochemical analysis. HMGB1 was abundantly expressed in the nuclei of the tumor cells and/or some of the tumor cell cytoplasms, and the expression was correlated with the result of 2DE and

Western blot analysis. We also demonstrated marked variation of HMGB1 expression in colorectal carcinomas. HMGB1 was originally identified as a chromosomal DNA-binding protein[49]. Apart from this intranuclear function, HMGB1 was also shown to be localized in the extracellular medium of different cell types as matrix-bound and to soluble molecules[50], and have an extracellular function in inflammation and tumor metastasis[51, 52]. Based on the reported function of HMGB1, the role of HMGB1 overexpression in GIST tumorigenesis can be explained in two ways. First, overexpressed HMGB1 can influence the expression and function of several related genes. HMGB1 is mainly localized in the nucleus and interacts with several transcription factors, by binding to the minor groove of DNA[52], increasing the binding affinity of several transcription factors[53] and down-regulating the binding affinity of p53 and p73 in the human *BAX* promoter[54]. Thus, we suggest that the overexpression of HMGB1 can contribute to tumorigenesis by altering tumor suppressor gene function. Second, HMGB1 directly activates signal transduction pathways related to cellular proliferation and/or metastasis. In addition to its intracellular role, HMGB1 is also secreted and/or released by certain cells, and plays important roles in tumor growth, invasion and metastasis[52]. Secreted and/or released HMGB1 binds to RAGE, as a receptor-ligand pair, and this complex activates several molecules, including mitogen activated protein kinase (MAPK) signaling molecules and MMPs. The suppression of tumor growth and metastasis by blocking RAGE-amphoterin (synonym of HMGB1) complex in mice had been reported. Therefore, it is likely that some of the overexpressed HMGB1 might exist in secreted forms or released forms after

necrosis, which are capable of facilitating tumor growth and metastasis. Although we could not confirm that a portion of the HMGB1 in our GISTs was in a secreted form, we demonstrated their presence by showing that MMP2 is selectively overexpressed according to HMGB1 expression in our GISTs. Taken together, our results suggest that overexpression of HMGB1 is related to the progression of GISTs.

We found several other proteins that are differently expressed according to tumor progression. Five proteins (Annexin V, HMGB1, C13orf2, Glutamate dehydrogenase 1, and Fibrinogen beta chain) were overexpressed in malignant GISTs compared to the benign GISTs, while, RoXaN protein levels were lower in malignant GISTs. Our findings suggest that differential protein expression may play a role in the different tumor development and progression of GISTs as these proteins are known to be involved in tumor metastasis, apoptosis, and tumor immune response, respectively.

Molecular mechanism of *KIT* and *PDGFRA* mutation and HMGB1 activation in the tumorigenesis of gastrointestinal tumors

Hyun Ju Kang

Department of Medical Science

The Graduate School, Yonsei University

(Directed by Professor Hoguen Kim)

CHAPTER II.

HMGB1 phosphorylation through the PKC signaling pathway and translocation mechanism in gastrointestinal tumors

I. INTRODUCTION

HMGB1 is one of several non-histone chromosomal proteins found in eukaryotic cells. The protein is typically located in the nucleus where it binds to minor groove DNA, promotes the assembly of site-specific DNA binding factors, and is involved in gene transcription[55-57]. In addition to transcriptional regulation, HMGB1 plays several well-established extracellular roles. HMGB1 localizes to the cell membrane of

neurites for outgrowth[58]. HMGB1 is secreted from activated monocytes, macrophages, and NK cells, and acts extracellularly as a proinflammatory cytokine.[59] It is passively secreted by necrotic cells, though not by apoptotic cells, and triggers inflammation[60, 61]. Recent studies have shown that the post-translational modification status of HMGB1 is related to *translocation* within cells and secretion by inflammatory cells, where it shuttles between the nucleus to the cytoplasm through hyperacetylation and phosphorylation in macrophages, and is monomethylated at Lys42 in neutrophils[55, 56, 62, 63]. Cytosolic HMGB1 accumulates and is secreted through a vesicle-mediated secretory pathway in monocytic cells[64, 65].

One important extracellular role of HMGB1 is the promotion of cell migration and metastasis[61, 66, 67]. We and others previously described the overexpression and cytoplasmic localization of HMGB1 in some tumor cells[68, 69]. These observations raise several additional questions: 1) How is HMGB1 in tumor cells transported from the nucleus to the cytoplasm? 2) If HMGB1 is transported to the cytoplasm and subsequently secreted from cancer cells, which signal triggers its movement? 3) If HMGB1 is secreted, does it contribute to cancer cell migration and metastasis?

To address these questions and we showed that phosphorylated HMGB1 localizes in the cytoplasm of colon cancer cells and that phosphorylation of HMGB1 is induced by the PKC-δ signaling pathway. HMGB1 is secreted from cancer cells, induces the MMP2 pathway and increases the invasiveness of these cancer cells. These findings suggest an autocrine and/or paracrine role of HMGB1 in cancer progression.

II. MATERIAL AND METHODS

1. Cell Lines and Tissue Samples

Cell lines were obtained from the American Type Culture Collection (ATCC; http://www.atcc.org) or the Korean Cell Line Bank (KCLB; http://cellbank.snu.ac.kr). Colo205, DLD-1, HCT116, HCT8, HT29, Ls174T, NCIH508, NCIH747, SNU-C4, SNU-C2A, and SW480 cells were grown in RPMI or DMEM medium supplemented with 10% fetal bovine serum (Life Technologies, Inc., Grand Island, NY, USA), at 37°C in the presence of 5% CO_2. CCD-18Co and RKO cells were cultured in minimal essential medium supplemented with 10% fetal bovine serum.

Eight colorectal carcinomas and matched normal mucosa were included in this study. All cases were identified in the Department of Pathology at Yonsei University Medical Center in September 1995 to November 2000. Some of the fresh specimens were supported by the Liver Cancer Specimen Bank from the National Research Resource Bank Program of the Korea Science and Engineering Foundation of the Ministry of Science and Technology. Authorization for the use of these tissues for research purposes was obtained from the Institutional Review Board of Yonsei University College of Medicine. To enrich for the tumor cell population, areas with more than 90% tumor cells were selected from hematoxylin-eosin stained slides using the cryostat microdissection technique.

2. Protein Extraction

Tumor tissues and matched non-tumorous tissues were suspended in ice-cold lysis buffer [50 mM Tris (pH 7.4), 1% Triton X-100, 5 mM EDTA, 1 mM KCl, 140 mM NaCl, 2 mM $MgCl_2$, 1 mM phenylmethylsulfonyl fluoride, 1 mM sodium fluoride, 1% aprotinin, 1 μM leupeptin, and 1 mM sodium ortho-vanadate] for 15 min. Suspensions were sonicated for approximately 30 sec and centrifuged at 20,000 x g for 15 min.

Four samples with sufficient material were selected for nuclear and cytoplasmic protein fractionation. Briefly, approximately 0.3 mg of frozen tissue was added 1 ml of buffer A [10 mM HEPES (N-2-hydroxyethylpiperrazine-N-2-ethanesulfonic acid) (pH 7.9), 10 mM KCl, 0.1 mM EDTA, 0.1 mM EGTA, 1 mM dithiothreitol, and 0.5 mM phenylmethylsulfonyl fluoride] and homogenized. The cells were allowed to swell on ice for 15 min, after which 50 μl of 10% NP-40 was added. After vigorous vortex for 10 sec, the homogenate was centrifuged for 30 sec. The supernatant was collected and used for cytoplasmic protein assays. The nuclear pellet was suspended in 100 μl of ice-cold buffer C [20 mM HEPES (pH 7.9), 0.4 mM NaCl, 1 mM EDTA, 1 mM EGTA, 1 mM dithiothreitol, and 1 mM phenylmethylsulfonyl fluoride] and shaken at 4°C for 15 min. Samples were then centrifuged for 5 min, and the supernatant was collected and used for nuclear protein assays.

3. Immunoblot and Immunoprecipitation Analysis

Forty μg of total protein lysate and cytoplasmic extracts and 5 μg of nuclear protein extracts were fractionated by SDS-PAGE. Proteins in the gel were transferred and blocked with TBS-T containing 5% skim milk. Anti-HMGB1 (BD Biosciences,

Franklin Lakes, NJ), anti-hnRNPC (Santa Cruz Biotechnology, Delaware Avenue, CA), anti-pan acetylation (Santa Cruz Biotechnology), anti-phosphoserine (BD Biosciences), anti-MMP2 (Calbiochem, Temecula, CA), anti-glyceraldehyde-3-phosphate dehydrogenase (GAPDH) (Trevigen, Gaithersburg, MD), anti-PKC (Santa Cruz Biotechnology), anti-PKC-α (Cell Signaling, Danvers, MA), anti-PKC-δ [61], anti-PKC-θ (Cell Signaling), anti-PKC-ζ (Cell Signaling), anti-RAGE (Santa Cruz Biotechnology), anti-Erk1/2 (Santa Cruz Biotechnology), and anti α-Tubulin (Oncogene, Cambridge, MA) were diluted 1:5,000 in blocking buffer and incubated for 1 h at room temperature. Membranes were washed and then incubated for 1 h with HRP-conjugated secondary antibody (Santa Cruz Biotechnology), washed, and developed with ECL-Plus (Amersham Pharmacia Biotech, Uppsala, Sweden). For immunoprecipitation experiments, 500 μg of tissue lysates were pre-cleared with PBS and gently rocked on an orbital shaker with anti-HMGB1 (BD Biosciences) at 4°C. The immune complexes were collected by centrifugation and boiled to dissociate the immunocomplexes from the beads. The beads were collected by centrifugation and protein separation was performed by SDS-PAGE with the supernatant fraction.

4. 2-Dimensional Electrophoresis (2-DE) Immunoblot Analysis

Colorectal carcinoma and matched normal tissues were suspended in sample buffer (40 mM Tris, 7 M urea, 2 M thiourea, 4% CHAPS, 100 mM 1, 4-dithioerythritol) and a protease inhibitor cocktail (Roche, Mannheim, Germany). Suspensions were sonicated for approximately 30 s and centrifuged at 100,000 x g for 45 min. One mg of total protein was used for each 2-DE analysis. Aliquots of proteins in sample buffer

were applied onto immobilized pH 3 to 10 non-linear gradient strips (Amersham Pharmacia Biotech, Uppsala, Sweden), and isoelectric focusing (IEF) was conducted at 100,000 Vh. Second dimension electrophoresis was performed in 9% to 16% linear gradient polyacrylamide gels (18 cm x 20 cm x 1.5 mm) as described previously[70], transferred to PVDF membranes, and subsequently blocked in TBS-T containing 5% skim milk. Anti-HMGB1 (BD Biosciences) was diluted 1:5,000 in blocking buffer and incubated with the membranes for 1 h at room temperature. After washing, membranes were incubated for 1 h with HRP-conjugated secondary antibody (Santa Cruz Biotechnology), washed, and developed with ECL-Plus (Amersham Pharmacia Biotech).

5. Vector Construction and Transfection

We performed transfection assays with 4 vectors (kindly provided by Dr. J-S Shin, Department of Microbiology, Yonsei University College of Medicine, Korea) 1) EGFPN1, used as a control, 2) NLS-WT, containing wild-type HMGB1, 3) NLS(1,2)-AT, containing HMGB1 sequence where the six serine residues in the NLS 1 and 2 regions were mutated to alanine for inhibition of HMGB1 phosphorylation, and 4) NLS(1,2)-ET, containing HMGB1 sequence where the six serine residues in the NLS 1 and 2 regions were mutated to glutamic acid for simulation of phosphorylated HMGB1[71].

Six vectors were constructed that contained serine to glutamic acid mutations in the NLS1 and NLS2 regions: NLS-35ET, NLS-39ET, NLS-42ET, NLS-46ET, NLS-

53ET, and NLS-181ET. One vector (NLS(1)-ET), contained serine to glutamic acid mutations of all 5 serine residues in the NLS1 region. An additional vector (NLS(1)-AT) contained serine to alanine mutations in all 5 serine residues. All the vectors were constructed using the QuikChange Site-Directed Mutagenesis Kit (Stratagene, La Jolla, CA), and sequences were confirmed by direct sequencing analysis (Figure 11A).

HCT116 Cell and CCD-18Co were transiently transfected using Lipofectamine 2000 (Invitrogen, Carlsbad, CA) with the constructed plasmid in a LabTek II chambers (Nalgene, Waltham, MA) or 60-mm tissue culture plate. Cells were observed or harvested 2 d later.

6. Immunofluorescence Imaging Analysis

Cells were cultured in LabTek II chambers (Nalgene) and fixed in 10% paraformaldehyde in PBS for 10 min at room temperature. The cells were then washed with PBS and incubated for 5 min at 4°C with permeabilization buffer containing 0.1% Triton X-100 in PBS. Samples were blocked with 2% BSA in PBS for 30 min and incubated with rabbit anti-HMGB1 for 1 h at room temperature. After three washes with 0.2% BSA in PBS, Alexa Fluor 488 secondary antibody (Invitrogen) was added. Mounting medium containing propidium iodide (Vector Laboratories, Burlingame, CA) was used. Fluorescently labeled cells were observed using the Zeiss LSM 510 confocal microscope (Carl Zeiss, Germany), and images were processed with LSM 5 Image Examiner software.

7. Drug Treatment

HCT116 cell lines were treated with kinase inhibitor Quercetin, Tamoxifen, Ly294002, or Myricetin (Calbiochem, Dermstadt, Germany), and CRM1-mediated active export inhibitor leptomycin B (Sigma-Aldrich, St. Louis, MO). We treated with myricetin at 3 μM or 10 μM, quercetin at 20 μM, tamoxifen at 6 μM and ly294002 at 1.4 μM. All drugs were dissolved in either distilled water or dimethyl sulfoxide (DMSO) and were added to the culture medium in volumes not exceeding 0.5% of the total culture medium volume.

8. Zymogram

HCT116 cells were transfected with each vector and the conditioned media were collected separately and analyzed for MMPs using Novex Zymogram gels (Invitrogen, Carlsbad, CA, USA). Protein lysates from the supernatants were collected in non-reducing buffer and were size-fractionated on a 10% zymogram gel. Gels were then incubated in renaturing buffer for 30 min and developed overnight. The gel was stained with Coomassie brilliant blue G-250 (Biorad, Hercules, CA). Areas of protease activity were detected as a clear band against a blue background and quantified using a densitometer.

9. Invasion Assay

The Cell Invasion Assay Kit (Chemicon International, Temecula, CA) was used according to the manufacturer's instructions. Briefly, the ECM layer was rehydrated

for 1-2 hours at room temperature with serum free medium. Five hundred µl of medium containing 10% fetal bovine serum was added to the lower chamber and prepared cell suspension in serum free medium was added to the upper chamber. Cells were incubated for 40 hours at 37°C in the presence of 5% CO_2. Noninvading cells were removed from the upper chamber and invasive cells on lower surface of the membrane were stained for 20 minutes. Invasiveness quantities by dissolving stained cells in 10% acetic acid and transfer a consistent amount of the dye/solute mixture to a 96 well plate for colorimetric reading of OD at 560 nm. Each experiment was performed in triplicate.

III. RESULTS

1. Overexpression and Cytoplasmic Localization of HMGB1 in Colon Cancer Cells

We first examined the amount of HMGB1 in eight colon cancer tissue samples and in normal mucosal tissues by immunoblot analysis. We found that HMGB1 was overexpressed in all colon cancer tissues tested. We also observed strong HMGB1 expression in 12 colon cancer cell lines, despite the variability between samples (Figure 9A). We then examined the level of nuclear and cytoplasmic HMGB1 by fractionation of nuclear and cytoplasmic proteins in four colon cancer tissues and normal mucosal tissues. The normal colonic fibroblast cell line, CCD-18Co, was used as a control. Strong HMGB1 expression was observed in both the nucleus and cytoplasm in all four colorectal carcinomas and in four colon cancer cell lines. The amount of nuclear HMGB1 in cancer cells, normal tissues, and normal fibroblast cell lines was not significantly different. However, cytoplasmic HMGB1 were absent or at low levels in normal tissues and normal fibroblast cell lines (Figure 9B and C), whereas cytoplasmic HMGB1 were found at high levels in tumor cells.

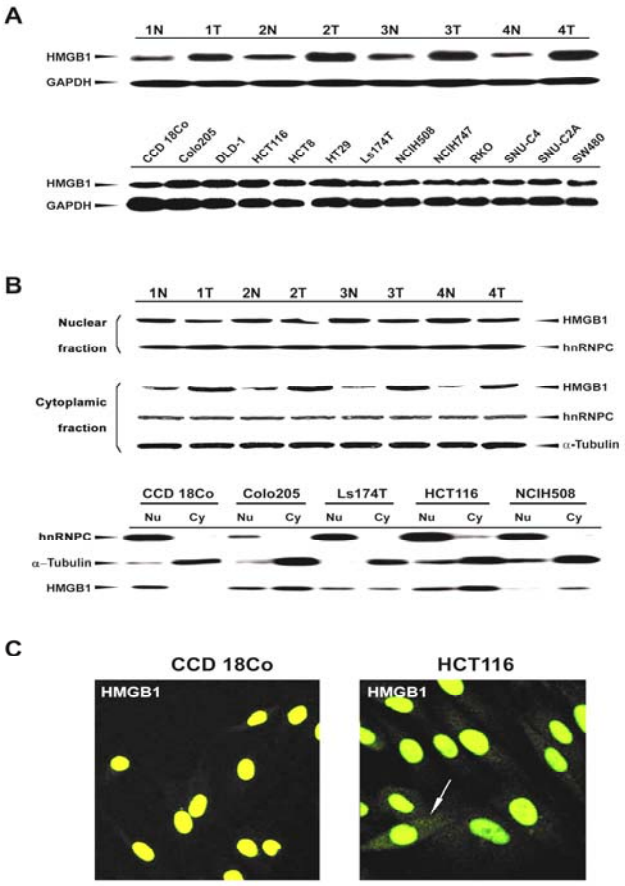

Figure 9. Overexpression and Nuclear and Cytoplasmic Localization of HMGB1 in Colon Cancer Cells. (*A*) HMGB1 expression in total protein lysates from four colon cancer samples, matched normal mucosal tissue samples, and 12 colon cancer cell lines. N, total protein lysate from normal colon tissue; T, total protein lysate from cancer tissue. (*B*) Analysis of HMGB1 expression in the nuclear and cytoplasmic protein fractions from four colon cancer tissues and five cell lines. Anti-hnRNPC was used for a nuclear protein control. Anti-tubulin was used for a cytoplasmic protein control. Nu, nuclear protein lysates; Cy, cytoplasmic protein lysates. (*C*) Localization of HMGB1 in CCD-18Co (normal) and HCT116 (cancerous) cell lines. Both nuclear and cytoplasmic localization (arrow) were evident in HCT116 cell line.

2. Identification of Cytoplasmic Phosphorylated HMGB1 in Cancer Cells

Because we observed that the intracellular distribution of HMGB1 differs between tumor and normal mucosa, we next compared the modification status of HMGB1 in these samples by 2-DE and Immunoblot analysis using HMGB1 antibody. Some spots with strong intensities in colon cancer samples had more acidic isoeletric points compared to those from the normal mucosa (Figure 10A). We next used prediction servers (http://www.cbs.dtu.dk/services/NetPhos/ and http://www.cbs.dtu.dk/services/NetAcet/) to predict of the modification status and found that phosphorylation and acetylation may occur in HMGB1. To validate any potential phosphorylation and acetylation modifications in HMGB1, we performed immunoprecipitation assays using protein lysates and an HMGB1 antibody followed by immunoblot analysis using antibodies against phosphorylated and acetylated proteins. We found that cells from both normal mucosa and cancer tissues contained acetylated HMGB1, but phosphorylated HMGB1 was only present in cancer cells (Figure 10B).

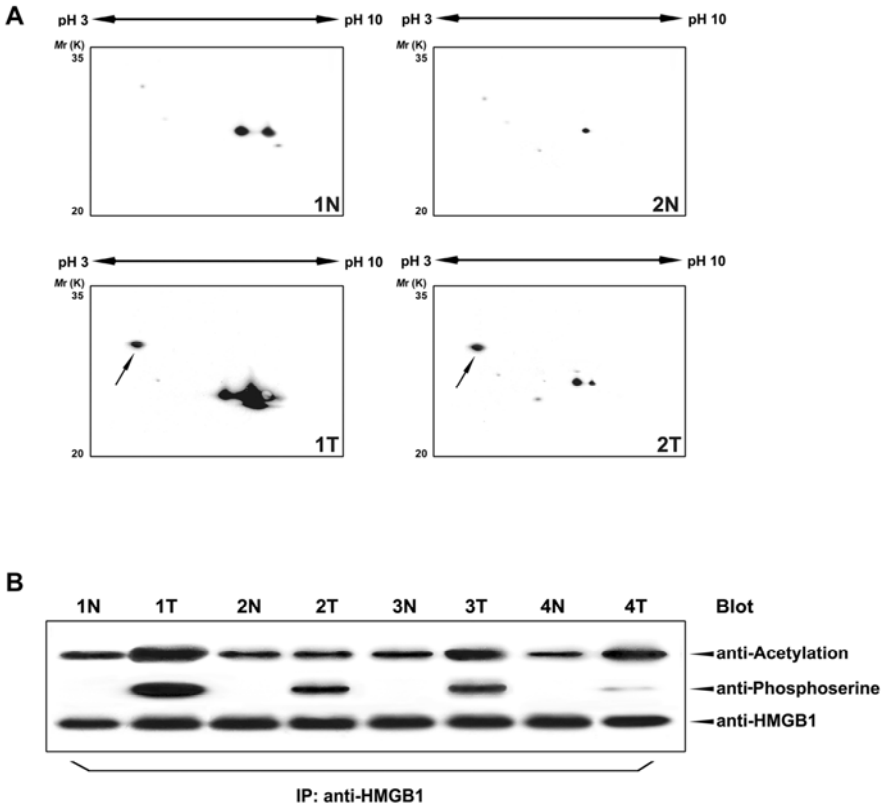

Figure 10. Identification of Cytoplasmic Phosphorylated HMGB1 in Cancer Cells. (*A*) 2-DE Immunoblot analysis with anti-HMGB1. Some HMGB1 spots with strong intensity in colon cancers reveal more acidic isoeletric points compared to normal mucosa (arrows). (*B*) Immunoprecipitation and immunoblot analysis with anti-acetylation and anti-phosphoserine. Both normal mucosa and cancer tissues contained acetylated HMGB1, but phosphorylated HMGB1 was only present in cancerous cells.

3. Cytoplasmic Transport of HMGB1 Is Related to Modification of Serine Residues in the Nuclear Localization Signal Sequence

Some reports have previously suggested that modified HMGB1 is related to its

cytoplasmic transport and secretion in inflammatory cells. In this study, we hypothesized that phosphorylation of HMGB1 is required for cytoplasmic transport in cancer cells. To test this hypothesis, we performed transfection assays with control and modified HMGB1 vectors to simulate the phosphorylation state of translocated HMGB1. We mutated serine residues within both of the nuclear localization signals (NLS) in HMGB1 to glutamic acid to simulate the phosphorylation status of the protein. We used four vectors in this experiment: 1) EGFPN1, used as a negative control, 2) NLS-WT, contains wild-type HMGB1 for overexpression of HMGB1, 3) NLS(1,2)-AT, contains HMGB1 sequence where six serine residues in NLS 1 and 2 were mutated to alanine for inhibition of HMGB1 phosphorylation, and 4) NLS(1,2)-ET, contains HMGB1 sequence where the six serine residues in NLS 1 and 2 were mutated to glutamic acid for simulation of phosphorylated HMGB1 (Figure 11A). When CCD-18Co cells were transfected with NLS(1,2)-AT or NLS-WT, HMGB1 was observed only in the nucleus. In contrast, high levels of HMGB1 were observed in the cytoplasm of CCD-18Co cells transfected with the NLS(1,2)-ET vector. In similar experiments using the colon cancer cell line HCT116, both nuclear and cytoplasmic HMGB1 was identified after transfection with NLS-WT, and HMGB1 was exclusively located in the nucleus after transfection with the NLS(1,2)-AT vector. In contrast, the majority of HMGB1 was located in the cytoplasm of HCT116 cells transfected with the NLS(1,2)-ET vector (Figure 11B). These results were confirmed by immunoblot of nuclear and cytoplasmic lysates (data not shown).

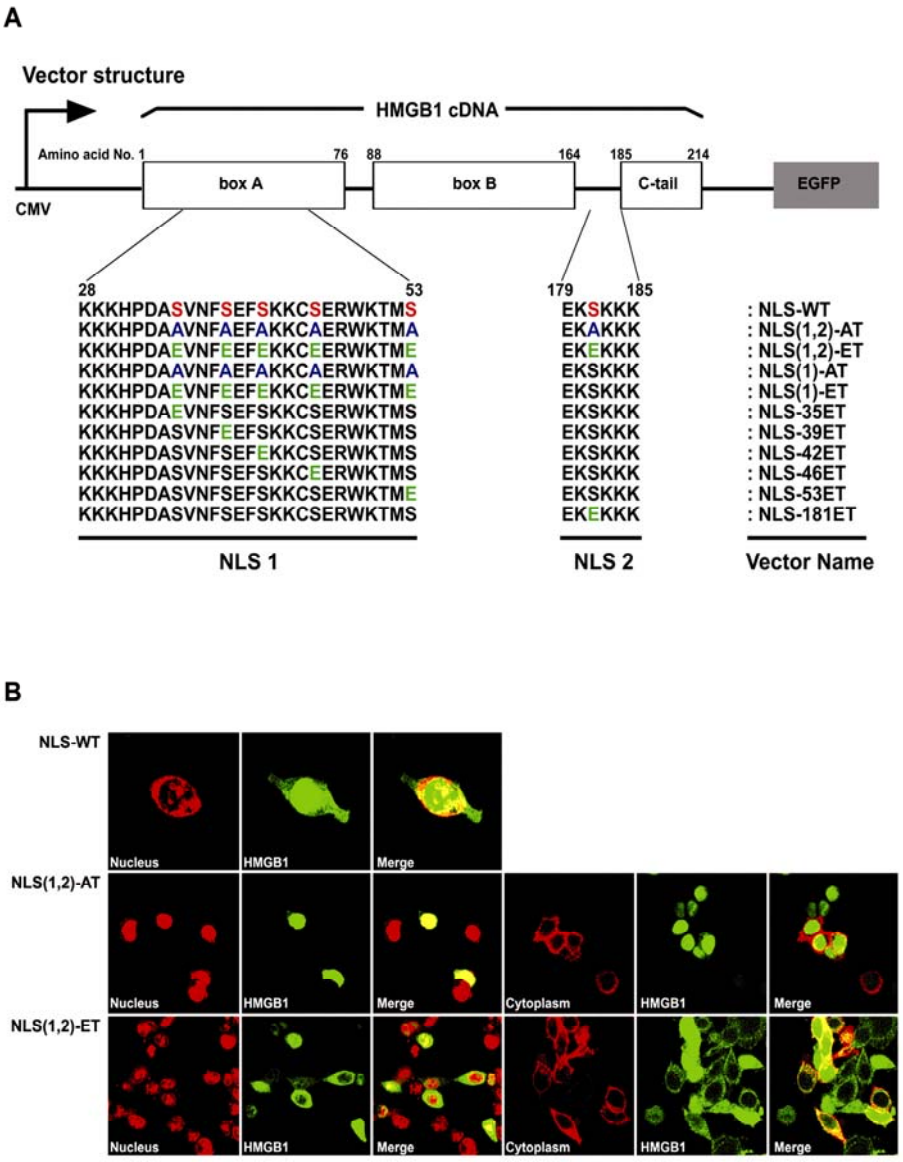

Figure 11. Cytoplasmic Transport and Secretion of HMGB1 is Related to the Modification of Serine Residues in the NLS. (*A*) Schematic diagram of HMGB1 gene structure and constructed vectors. HMGB1 consists of two DNA-binding domains, the HMG boxes A and B, and an acidic C-terminal domain. The A-box and B-box both contain nuclear localization signals (NLS) NLS1, which includes amino acids 28-53, and NLS2, which includes amino acids 179-

185. A description of each vector can be found in the text. (*B*) Localization of HMGB1 in HCT116 cells transfected with NLS-WT, NLS(1,2)-AT, or NLS(1,2)-ET. Cytoplasmic HMGB1 was evident in the cell lines transfected with NLS-WT and NLS(1,2)-ET.

4. Phosphorylation of Serine 35, 39 and 42 Are Critical for Nucleus to Cytoplasmic HMGB1 Transport

To identify which of the six serine residues in the NLS 1 and 2 regions is critical for HMGB1 transport from the nucleus to the cytoplasm, we constructed six HMGB1 vectors (NLS-35ET, NLS-39ET, NLS-42ET, NLS-46ET, NLS-53ET and NLS-181ET), each containing a serine to glutamic acid mutation at the residue indicated (Figure 11A). We also constructed one vector (NLS(1)-ET) where all five serine residues in the NLS1 region were mutated to glutamic acid. The matched vector NLS(1)-AT was also constructed, where all five serine residues were converted to alanine. In this transfection study, we observed that only cells transfected with NLS(1)-ET, NLS-35ET, NLS-39ET and NLS-42ET showed increased HMGB1 transport from the nucleus to the cytoplasm as compared to cells transfected with the other three vectors (Figure 12), suggesting that serine residues at 35, 39 and 42 are important for HMGB1 transport.

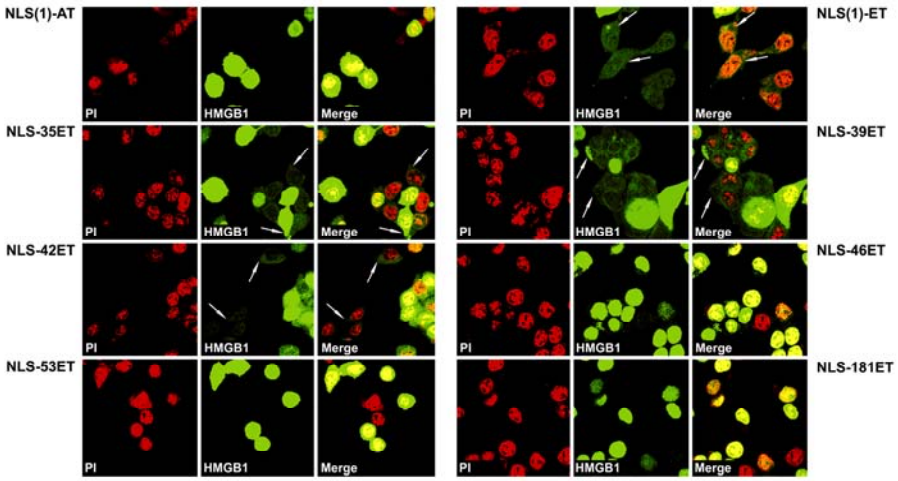

Figure 12. Phosphorylation of Serine 35, 39 and 42 is Critical for Cytoplasmic Localization of HMGB1. Cytoplamic HMGB1 (arrows) is found in the HCT116 cells transfected with NLS(1)-ET (vector where all five serine residues in the NLS1 region were mutated to glutamic acid), NLS-35ET, NLS-39ET and NLS-42ET (containing a serine to glutamic acid mutation at the residue indicated Figure 11*A*).

5. HMGB1 Phosphorylation through the PKC Signaling Pathway

In order to identify which factors responsible for HMGB1 phosphorylation, we used the NetPhosK 1.0 server (http://www.cbs.dtu.dk/services/NetPhosK/) to identify kinases that could potentially bind to and induce phosphorylation of HMGB1. We identified casein kinase 1 (CK1) and PKC as possible candidates. We next performed a kinase inhibitor study to test which factor was involved in HMGB1 phosphorylation. We used Quercetin to inhibit CK1, and Tamoxifen and Ly294002 to inhibit PKC. We also used Myricetin at both 3 μM and 10 μM, as it has been reported to inhibit CK1 or

PKC at low or high concentrations, respectively. The distribution of HMGB1 did not change in HCT116 cells treated with Quercetin or with 3 μM Myricetin, indicating that CK1 was not involved in HMGB1 translocation. In contrast, HMGB1 expression in the cytoplasm was significantly decreased in cells treated with Tamoxifen or Ly294002 (Figure 13A). Decreased cytoplasmic expression of HMGB1 was also observed in cells treated with 10 μM Myricetin. The requirement for PKC was validated by immunoprecipitation analysis to test of co-interaction between PKC and HMGB1 (Figure 13B). These findings indicate that PKC signaling is directly involved in the cytoplasmic translocation of HMGB1 in colorectal cancer cells.

6. Nuclear PKC-δ Induces HMGB1 Phosphorylation

We analyzed which isoform(s) among the PKC family was involved in HMGB1 phosphorylation. We performed immunoblot analysis using the PKC-α, PKC-δ, PKC-θ and PKC-ζ antibodies. In our immunoblot analysis, we observed that only the PKC-δ and PKC-ζ expressed in the nucleus. PKC-α was only detected in the cytoplasm and PKC-θ is not detected in the colon cancer cells (Figure 14A). In order to identify the interaction between PKC and HMGB1 in the nucleus, we performed immunoprecipitation assays using a HMGB1 antibody. Immunoblot analysis was performed with antibodies against PKC-δ and PKC-ζ. We found that PKC-δ is directly interacted with nuclear HMGB1 (Figure 14B). In contrast, no interaction between PKC-ζ and nuclear HMGB1 was found. These findings indicate that PKC-δ is directly involved in the phosphorylation of nuclear HMGB1.

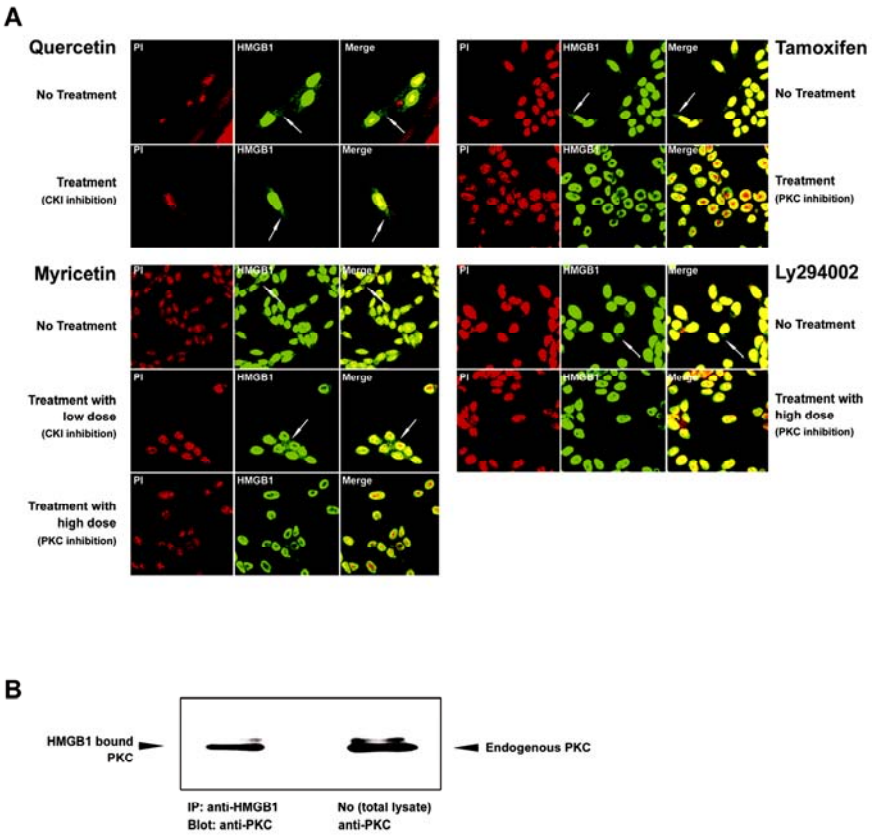

Figure 13. PKC Induces HMGB1 Phosphorylation. (*A*) The distribution of HMGB1 did not change with treatment of CK1 inhibitors; Quercetin or low dose (3 μM) of Myricetin treatment. HMGB1 expression in the cytoplasm is significantly decreased in treatment of PKC inhibitors; Tamoxifen or Ly294002 treatment in HCT116 cells. Increased cytoplasmic expression was also found in a high dose (10 μM) of Myricetin treatment, one of PKC inhibitor. (*B*) Verification of the binding of PKC and HMGB1 by immunoprecipitation analysis in HCT116 cell line. Binding of PKC and HMGB1 was noted.

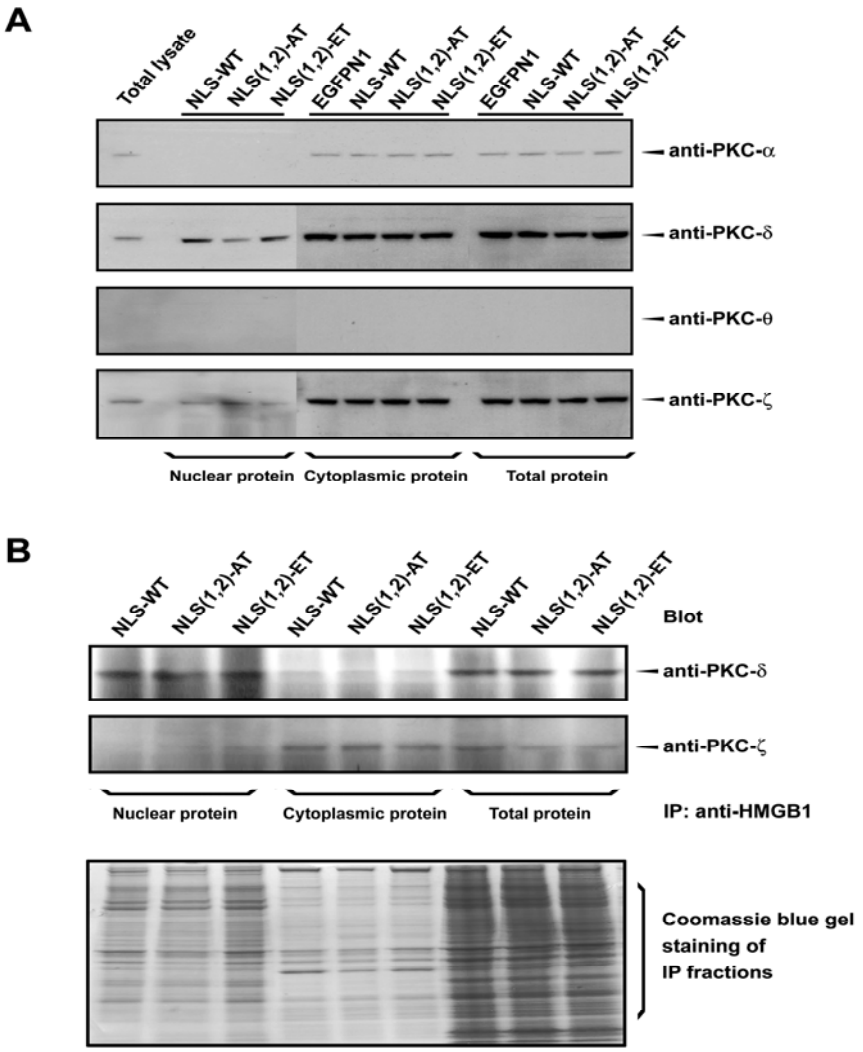

Figure 14. Nuclear PKC-δ Induces HMGB1 Phosphorylation. (*A*) Analysis of PKC expression in the nuclear and cytoplasmic protein fractions from transfected cells with EGFPN1, NLS-WT, NLS(1,2)-AT and NLS(1,2)-ET vectors. PKC-δ and PKC-ζ were only present in nucleus. In contrast, PKC-α was only detected in the cytoplasm and PKC-θ is not detected in the colon cancer cells. (*B*) Immunoblot analysis with PKC-δ and PKC-ζ after immunoprecipitation with HMGB1. Direct interaction of PKC-δ and nuclear HMGB1 was found. In contrast, no interaction between PKC-ζ and nuclear HMGB1 was found.

7. HMGB1 Is Unidirectional Transported from the Nucleus to the Cytoplasm

HMGB1 is a small molecule and has the potential to migrate from the nucleus to the cytoplasm by simple diffusion across nuclear pores. To test if the translocation of HMGB1 from the nucleus to the cytoplasm is unidirectional in a chromosome region maintenance 1 (CRM1)-dependent manner, or if it is bidirectional by simple diffusion, we treated HCT116 cells with leptomycin B, an inhibitor of CRM1-mediated active export. We found that endogenous cytoplasmic HMGB1 was markedly decreased after treatment of Leptomycine B, indicating that cytoplasmic translocation of HMGB1 was unidirectional and conducted through active transport (Figure 15).

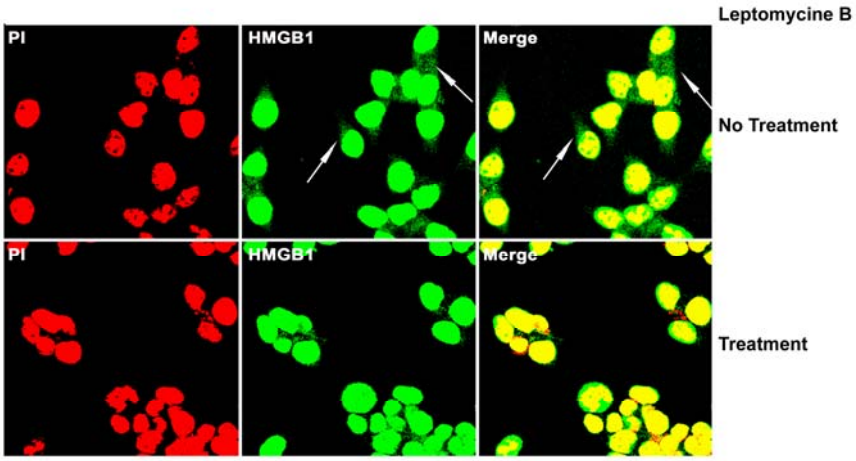

Figure 15. Inhibition of CRM1-mediated HMGB1 transport by leptomycin B treatment. Endogenous HMGB1 is noted in cancer cell cytoplasm (arrows), however markedly decreased after treatment of leptomycin B.

8. Secretion of HMGB1 is related to increased tumor cell invasiveness

The results described above predict that modified HMGB1 is secreted into the extracellular space. To confirm this idea we measured the amount of HMGB1 by immunoblot in the culture medium from cells transfected with the vectors described above. A relatively large amount of HMGB1 was detected in the culture medium of HCT116 cells transfected with the NLS-WT or NLS(1,2)-ET vectors. In contrast, scant amounts of HMGB1 were noted in the medium from cells transfected with the NLS(1,2)-AT vector (Figure 16A). To verify the phosphorylation status of HMGB1 in the culture medium, we performed immunoprecipitation experiments using media protein and an HMGB1 antibody, followed by immunoblot analysis using antibodies against phosphorylated proteins. We found that phosphorylated HMGB1 was present in the culture medium of cancer cells (Figure 16B). These findings indicate that phosphorylated HMGB1 is transported to the cytoplasm and subsequently secreted into the extracellular space.

To extend these observations to tumor cell invasiveness, we next tested if phosphorylated HMGB1 could activate signal transduction pathways related to cell migration and metastasis. We next measured MMP activity in the culture medium. We found that MMP9 activity did not differ between the four cell lines transfected with different vectors. However, MMP2 activity was increased in HCT116 cells transfected with NLS(1,2)-ET as compared to cells transfected with the other vectors [NLS-WT, NLS(1,2)-AT, and EGFPN1] (Figure 16C).

We performed the invasion assay using tissue culture plate containing an 8 μm pore size polycarbonate membrane which blocked non-invasive cells from migrating

through. Invasive cells, on the other hand, migrate through the layer and cling to the bottom of the polycarbonate membrane. We found that the invasiveness was markedly increased in cells transfected with NLS(1,2)-ET and slightly increased in cells transfected with NLS-WT. Cells transfected with NLS(1,2)-AT or the control vector showed low invasion activity compared to cells transfected with NLS-WT or NLS(1,2)-ET (Figure 15C). To ascertain the role of secreted HMGB1, we treated cells with recombinant HMGB1 by including it in the culture medium, and found that invasiveness was markedly increased in HCT116 cells (Figure 16D). These findings indicate that phosphorylated HMGB1 is directly related to increased MMP2 activity and to cell invasion capacity.

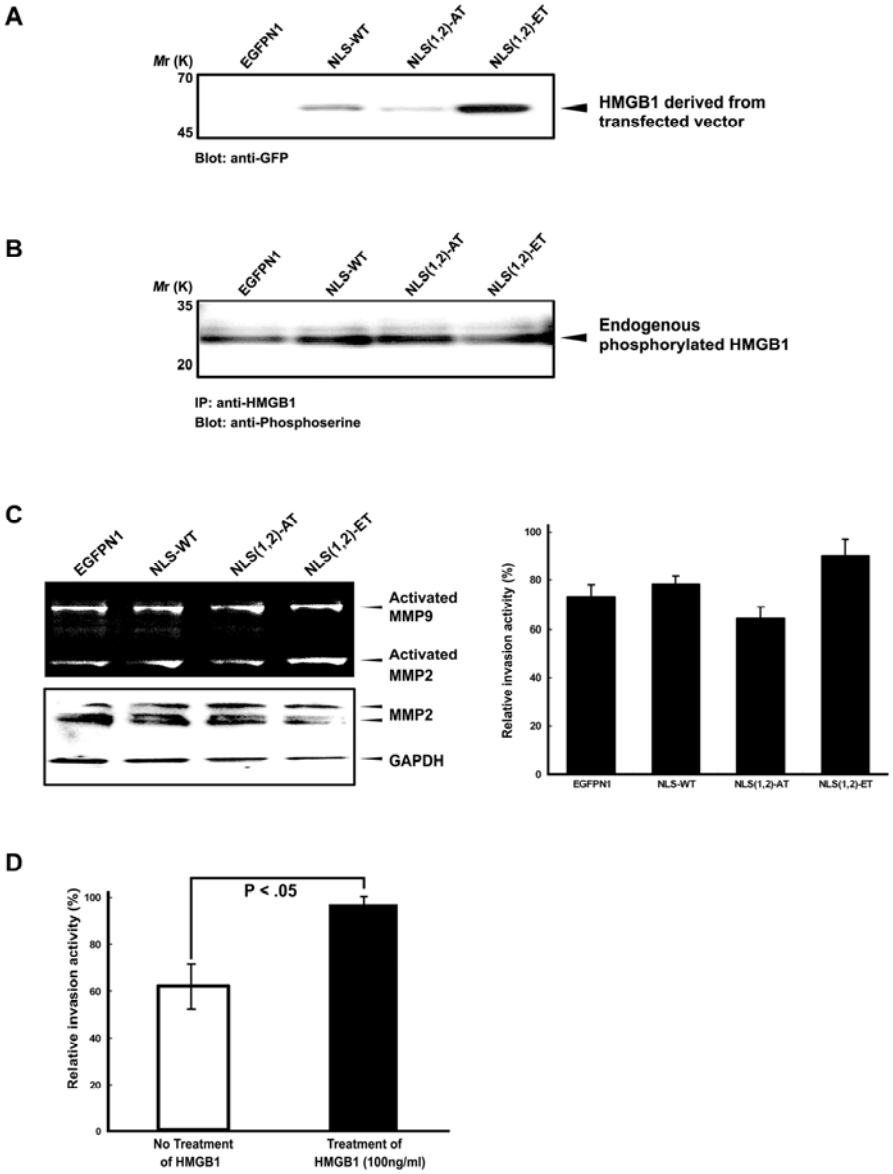

Figure 16. Extracellular HMGB1 Activate MMP2 Pathways and Promote Cell Invasion. (*A*) Immunoblot analysis of HMGB1 from the culture medium of HCT116 cells transfected with NLS-WT, NLS(1,2)-AT, or NLS(1,2)-ET vectors. Secreted HMGB1 was evident in the cell lines transfected with NLS-WT and NLS(1,2)-ET. (*B*) Immunoprecipitation of media protein lysates using HMGB1 antibody and immunoblot using antibodies against phosphorylated

proteins. Similar amount of endogenous phosphorylated HMGB1 was found in all of 4 cell lines transfected with different vectors. (*C*) No difference in the protein expression level of MMP2 and activated MMP9 was noted between 4 cell lines transfected with EGFPN1, NLS-WT, NLS(1,2)-AT and NLS(1,2)-ET vectors. However, MMP2 activity and invasion activity are increased in HCT116 cells transfected with NLS(1,2)-ET vector than in cells transfected with other forms of vectors (NLS-WT, NLS(1,2)-AT and EGFPN1). (*D*) Treatment of recombinant HMGB1 protein in the culture media demonstrated increased invasiveness of tumor cells.

IV. DISCUSSION

In this study, we demonstrated overexpression of HMGB1 in cancer cells, cytoplasmic transport of HMGB1, the presence of extracellular HMGB1, PKC-δ mediated HMGB1 phosphorylation, activation of the MMP2 pathway, and increased cell invasion after transfection of activated HMGB1. These findings suggest that HMGB1 indeed plays a role in the ability of cancer cells to invade surrounding tissue and metastasis.

One of the important roles of HMGB1 is cell migration and metastasis in cancer cells involves activation of RAGE and the MMP2 pathway[56, 66, 72]. It has been proposed that secreted HMGB1 from both inflammatory and necrotic cells play a role in this signal transduction event[73-77]. In this study, we demonstrated that endogenous HMGB1 can be secreted into the extracellular space, where it can bind to RAGE and activate the MMP2 pathway. Our novel finding that endogenous HMGB1 can cause aberrant signaling events in cancer cells partially explains the early phase of cancer metastasis. Metastasis is a complicated and multistep process. Little is known about the mechanism by which cancer cells acquire invasion and cell migration ability. Here we suggest that signals required for metastasis can be initiated by the cancer cell itself through autocrine and/or paracrine activation by secreted HMGB1.

Our data suggest that the nuclear and/or cytosolic distribution of HMGB1 is caused by protein phosphorylation. We propose that the cytoplasmic transport of HMGB1 is the result of its phosphorylation. It has been shown that phosphorylation of HMGB1 leads to more negatively charged groups on the protein, reducing its DNA binding

activity by up to 10-fold[78, 79]. We confirmed that the reduced DNA-binding affinity of HMGB1 enables its cytoplasmic transport. We modified the serine residues in two NLS regions of HMGB1 to glutamic acid (NLS(1,2)-ET) in order to simulate phosphorylation and to alanine (NLS(1,2)-AT) to prevent phosphorylation. Cells transfected with the NLS(1,2)-ET vector showed increased cytoplamic HMGB1 transport, while HMGB1 was retained in the nucleus in cells transfected with the NLS(1,2)-AT vector. These findings indicate that the negatively charged status of HMGB1 was directly related to cytoplasmic transport. Moreover, our CRM1 inhibition study demonstrated marked reduction of endogenous cytoplasmic HMGB1. This indicates that HMGB1 is translocated from the nucleus to the cytoplasm by active transport rather than by simple diffusion, and implies that HMGB1 phosphorylation occurs in the nucleus. These findings also suggest that a signal transduction pathway activated in these cancer cells regulates the translocation of endogenous HMGB1.

Our results suggest that HMGB1 phosphorylation is induced by PKC. PKC binds to HMGB1 and PKC inactivation results in decreased HMGB1 phosphorylation. Additionally, phosphorylation of serines 35, 39 and 42 of the NLS1 region in HMGB1 is critical for HMGB1 transport into the cytoplasm, and these serine residues are consistent with the predicted PKC binding site. The PKC family consists of at least 12 serine-threonine kinases that are classified into three major groups[80, 81], and their expression level was variable according to cancer type. The most important and well known cancer-related targets of PKC are Erk1/2, glycogen synthase kinase 3 beta

(GSK-3β), nuclear factor kappa B (NFκB), and P-glycoprotein[82, 83]. Previous reports demonstrated that the biological functions of PKC are mostly linked to events occurring at the plasma membrane or in the cytoplasm. PKC isoforms are thought to reside in the cytoplasm in an inactive state, translocated to the plasma membrane after stimulation, and become activated in the presence of specific co-factors[84-87]. However, some reports indicate that PKC isoforms are located in the nucleus or are translocated to the nucleus. Likewise, other reports suggest a direct relationship between nuclear PKC and tumorigenesis[88-91], although the regulatory role of nuclear PKC in cancer is not completely understood[88-93]. In this study, we demonstrated that HMGB1 interacted with PKC-δ in the nucleus. Our findings suggest that nuclear PKC-δ induces HMGB1 phosphorylation, and phosphorylated HMGB1 plays a role in tumor progression through the activation of genes related to cell invasion.

In conclusion, we demonstrated that nuclear HMGB1 is phosphorylated and that phosphorylated HMGB1 can be secreted into the extracellular space. Phosphorylated HMGB1 then induces migration of the cancer cells. These findings suggest that cancer cells can acquire the ability to invade surrounding tissues and to metastasize through activation of endogenous nuclear HMGB1.

V. CONCLUSION

1. Unsupervised clustering analysis demonstrates that gene expressions of GISTs are different according to mutation status of *KIT* or *PDGFRA*.

2. Mutation of *KIT* and *PDGFRA* are directly correlated to the overexpression of active KIT and PDGFRA

3. The mutation status of *KIT* or *PDGFRA* is directly related to the expression levels of activated KIT and PDGFRA, and is also related to the different expression levels of activated proteins that play key roles in the downstream of the receptor tyrosine kinase III family.

4. 2DE expression analysis shows that the expression of some protein is different according to the mutation status and tumor grade in GISTs.

5. HMGB1 is overexpressed and translocated from nucleus to cytoplasm in colon cancer cell

6. Cells from both normal mucosa and cancer tissue contain acetylated HMGB1, but phosphorylated HMGB1 is only present in cancer cells.

7. Phosphorylated HMGB1 localizes in the cytoplasm of colon cancer cells and phosphorylation of serine 35, 39 and 42 are critical for nucleus to cytoplasmic transport.

8. HMGB1 is induced phosphorylation through the PKC signaling pathway in nucleus and phosphorylated HMGB1 can be secreted into the extracellular space.

9. Secretion of HMGB1 is related to the activation of the Erk1/2 and MMP2 pathways and to increased tumor cell invasiveness

IV. REFERENCES

1. Schlessinger J. Cell signaling by receptor tyrosine kinases. Cell 2000;103:211-25.
2. Hunter T. The Croonian Lecture 1997. The phosphorylation of proteins on tyrosine: Its role in cell growth and disease. Philos T Roy Soc B 1998;353:583-605.
3. Hanahan D, Weinberg RA. The hallmarks of cancer. Cell 2000;100:57-70.
4. Resnik JL, Reichart DB, Huey K, Webster NJG, Seely BL. Elevated insulin-like growth factor I receptor autophosphorylation and kinase activity in human breast cancer. Cancer Res 1998;58:1159-64.
5. Heldin CH. Signal transduction: Multiple pathways, multiple options for therapy. Stem Cells 2001;19:295-303.
6. Blume-Jensen P, Hunter T. Oncogenic kinase signalling. Nature 2001;411:355-65.
7. Fletcher CDM. Clinicopathologic correlations in gastrointestinal stromal tumors. Hum Pathol 2002;33:455-.
8. Fletcher JA, Fletcher CDM, Rubin BP, Ashman LK, Corless CL, Heinrich MC. KIT gene mutations in gastrointestinal stromal tumors - More complex than previously recognized? Am J Pathol 2002;161:737-8.
9. Hirota S, Isozaki K, Moriyama Y, Hashimoto K, Nishida T, Ishiguro S, et al. Gain-of-function mutations of *c-kit* in human gastrointestinal stromal tumors. Science 1998;279:577-80.

10. Lasota J, Jasinski M, Miettinen M. Mutations in exon 11 of *c-kit* occur preferentially in malignant vs. benign gastrointestinal stromal tumors (GISTs). Lab Invest 1999;79:78a-a.

11. Lasota J, Jasinski M, Sarlomo-Rikala M, Miettinen M. Mutations in exon 11 of *c-kit* occur preferentially in malignant versus benign gastrointestinal stromal tumors and do not occur in leiomyomas or leiomyosarcomas. Am J Pathol 1999;154:53-60.

12. Miettinen M, Sarlomo-Rikala M, Lasota J. Gastrointestinal stromal tumors: Recent advances in understanding of their biology. Hum Pathol 1999;30:1213-20.

13. Taniguchi M, Nishida T, Hirota S, Isozaki K, Ito T, Nomura T, et al. Effect of *c-kit* mutation on prognosis of gastrointestinal stromal tumors. Cancer Res 1999;59:4297-300.

14. Hirota S, Ohashi A, Nishida T, Isozaki K, Kinoshita K, Shinomura Y, et al. Gain-of-function mutations of *platelet-derived growth factor receptor alpha* gene in gastrointestinal stromal tumors. Gastroenterology 2003;125:660-7.

15. Pawson T, Gish GD, Nash P. SH2 domains, interaction modules and cellular wiring. Trends Cell Biol 2001;11:504-11.

16. Heinrich MC, Corless CL, Duensing A, McGreevey L, Chen CJ, Joseph N, et al. *PDGFRA* activating mutations in gastrointestinal stromal tumors. Science 2003;299:708-10.

17. West RB, Corless CL, Chen X, Rubin BP, Subramanian S, Montgomery K, et al. The novel marker, DOG1, is expressed ubiquitously in gastrointestinal stromal tumors irrespective of *KIT* or *PDGFRA* mutation status. Am J Pathol 2004;165:107-13.

18. Subramanian S, West RB, Corless CL, Ou WB, Rubin BP, Chu KM, et al. Gastrointestinal stromal tumors (GISTs) with *KIT* and *PDGFRA* mutations have distinct gene expression profiles. Oncogene 2004;23:7780-90.

19. Lux ML, Rubin BP, Biase TL, Chen CJ, Maclure T, Demetri G, et al. *KIT* extracellular and kinase domain mutations in gastrointestinal stromal tumors. Am J Pathol 2000;156:791-5.

20. Rubin BP, Singer S, Tsao C, Duensing A, Lux ML, Ruiz R, et al. KIT activation is a ubiquitous feature of gastrointestinal stromal tumors. Cancer Res 2001;61:8118-21.

21. Joseph S, Weiser B, Noller HF. Mapping the inside of the ribosome with an RNA helical ruler. Science 1997;278:1093-8.

22. Raychaudhuri S, Stuart JM, Altman RB. Principal components analysis to summarize microarray experiments: application to sporulation time series. Pac Symp Biocomput 2000:455-66.

23. Lasota J, Jasinski M, Sarlomo-Rikala M, Miettinen M. Mutations in exon 11 of *c-Kit* occur preferentially in malignant versus benign gastrointestinal stromal tumors and do not occur in leiomyomas or leiomyosarcomas. Am J Pathol 1999;154:53-60.

24. Taniguchi M, Nishida T, Hirota S, Isozaki K, Ito T, Nomura T, et al. Effect of *c-kit* mutation on prognosis of gastrointestinal stromal tumors. Cancer Res 1999;59:4297-300.

25. Lux ML, Rubin BP, Biase TL, Chen CJ, Maclure T, Demetri G, et al. *KIT* extracellular and kinase domain mutations in gastrointestinal stromal tumors. Am J Pathol 2000;156:791-5.

26. Heinrich MC, Corless CL, Duensing A, McGreevey L, Chen CJ, Joseph N, et al. *PDGFRA* activating mutations in gastrointestinal stromal tumors. Science 2003;299:708-10.

27. Hirota S, Ohashi A, Nishida T, Isozaki K, Kinoshita K, Shinomura Y, et al. Gain-of-function mutations of *platelet-derived growth factor receptor alpha* gene in gastrointestinal stromal tumors. Gastroenterology 2003;125:660-7.

28. Blume-Jensen P, Hunter T. Oncogenic kinase signalling. Nature 2001;411:355-65.

29. Pawson T. Regulation and targets of receptor tyrosine kinases. Eur J Cancer 2002;38 Suppl 5:S3-10.

30. Allander SV, Nupponen NN, Ringner M, Hostetter G, Maher GW, Goldberger N, et al. Gastrointestinal stromal tumors with *KIT* mutations exhibit a remarkably homogeneous gene expression profile. Cancer Res 2001;61:8624-8.

31. Nielsen OS, O'Sullivan B. Retroperitoneal soft tissue sarcomas: a treatment challenge and a call for randomized trials. Radiother Oncol 2002;65:133-6.

32. Kim NG, Kim JJ, Ahn JY, Seong CM, Noh SH, Kim CB, et al. Putative chromosomal deletions on 9P, 9Q and 22Q occur preferentially in malignant gastrointestinal stromal tumors. Int J Cancer 2000;85:633-8.

33. El-Rifai W, Sarlomo-Rikala M, Andersson LC, Knuutila S, Miettinen M. DNA sequence copy number changes in gastrointestinal stromal tumors: tumor progression and prognostic significance. Cancer Res 2000;60:3899-903.

34. Antonescu CR, Viale A, Sarran L, Tschernyavsky SJ, Gonen M, Segal NH, et al. Gene expression in gastrointestinal stromal tumors is distinguished by *KIT* genotype and anatomic site. Clin Cancer Res 2004;10:3282-90.

35. Weiler SR, Mou S, DeBerry CS, Keller JR, Ruscetti FW, Ferris DK, et al. JAK2 is associated with the c-kit proto-oncogene product and is phosphorylated in response to stem cell factor. Blood 1996;87:3688-93.

36. Schindler C, Darnell JE, Jr. Transcriptional responses to polypeptide ligands: the JAK-STAT pathway. Annu Rev Biochem 1995;64:621-51.

37. Brizzi MF, Rossi PR, Rosso A, Avanzi GC, Pegoraro L. Transcriptional and post-transcriptional regulation of granulocyte-macrophage colony-stimulating factor production in human growth factor dependent M-07e cells. Br J Haematol 1995;90:258-65.

38. Burack WR, Sturgill TW. The activating dual phosphorylation of MAPK by MEK is nonprocessive. Biochemistry 1997;36:5929-33.

39. Barker SA, Caldwell KK, Pfeiffer JR, Wilson BS. Wortmannin-sensitive phosphorylation, translocation, and activation of PLCgamma1, but not PLCgamma2, in antigen-stimulated RBL-2H3 mast cells. Mol Biol Cell 1998;9:483-96.

40. Zhang S, Coso OA, Collins R, Gutkind JS, Simonds WF. A C-terminal mutant of the G protein beta subunit deficient in the activation of phospholipase C-beta. J Biol Chem 1996;271:20208-12.

41. Timokhina I, Kissel H, Stella G, Besmer P. Kit signaling through PI 3-kinase and Src kinase pathways: an essential role for Rac1 and JNK activation in mast cell proliferation. EMBO J 1998;17:6250-62.

42. Schlessinger J. Cell signaling by receptor tyrosine kinases. Cell 2000;103:211-25.

43. Miettinen M, Paal E, Lasota J, Sobin LH. Gastrointestinal glomus tumors: a clinicopathologic, immunohistochemical, and molecular genetic study of 32 cases. Am J Surg Pathol 2002;26:301-11.

44. Nagata K, Inagaki M. Cytoskeletal modification of Rho guanine nucleotide exchange factor activity: identification of a Rho guanine nucleotide exchange factor as a binding partner for Sept9b, a mammalian septin. Oncogene 2005;24:65-76.

45. Conroy SE, Latchman DS. Do heat shock proteins have a role in breast cancer? Br J Cancer 1996;74:717-21.

46. Jolly C, Morimoto RI. Role of the heat shock response and molecular chaperones in oncogenesis and cell death. J Natl Cancer Inst 2000;92:1564-72.

47. Paul C, Manero F, Gonin S, Kretz-Remy C, Virot S, Arrigo AP. Hsp27 as a negative regulator of cytochrome C release. Mol Cell Biol 2002;22:816-34.

48. Lebret T, Watson RW, Fitzpatrick JM. Heat shock proteins: their role in urological tumors. J Urol 2003;169:338-46.

49. Bustin M. Regulation of DNA-dependent activities by the functional motifs of the high-mobility-group chromosomal proteins. Mol Cell Biol 1999;19:5237-46.

50. Passalacqua M, Zicca A, Sparatore B, Patrone M, Melloni E, Pontremoli S. Secretion and binding of HMG1 protein to the external surface of the membrane are required for murine erythroleukemia cell differentiation. FEBS Lett 1997;400:275-9.

51. Wang H, Bloom O, Zhang M, Vishnubhakat JM, Ombrellino M, Che J, et al. HMG-1 as a late mediator of endotoxin lethality in mice. Science 1999;285:248-51.

52. Muller S, Scaffidi P, Degryse B, Bonaldi T, Ronfani L, Agresti A, et al. New EMBO members' review: the double life of HMGB1 chromatin protein: architectural factor and extracellular signal. EMBO J 2001;20:4337-40.

53. Bianchi ME, Beltrame M. Upwardly mobile proteins. Workshop: the role of HMG proteins in chromatin structure, gene expression and neoplasia. EMBO Rep 2000;1:109-14.

54. Stros M, Ozaki T, Bacikova A, Kageyama H, Nakagawara A. HMGB1 and HMGB2 cell-specifically down-regulate the p53- and p73-dependent sequence-specific transactivation from the human Bax gene promoter. J Biol Chem 2002;277:7157-64.

55. Bonaldi T, Langst G, Strohner R, Becker PB, Bianchi ME. The DNA chaperone HMGB1 facilitates ACF/CHRAC-dependent nucleosome sliding. Embo J 2002;21:6865-73.

56. Pallier C, Scaffidi P, Chopineau-Proust S, Agresti A, Nordmann P, Bianchi ME, et al. Association of chromatin proteins high mobility group box (HMGB) 1 and HMGB2 with mitotic chromosomes. Mol Biol Cell 2003;14:3414-26.

57. Stros M, Ozaki T, Bacikova A, Kageyama H, Nakagawara A. HMGB1 and HMGB2 cell-specifically down-regulate the p53-and p73-dependent sequence-specific transactivation from the human Bax gene promoter. J Biol Chem 2002;277:7157-64.

58. Fages C, Nolo R, Huttunen HJ, Eskelinen EL, Rauvala H. Regulation of cell migration by amphoterin. J Cell Sci 2000;113:611-20.

59. Lotze MT, Tracey KJ. High-mobility group box 1 protein (HMGB): Nuclear weapon in the immune arsenal. Nat Rev Immunol 2005;5:331-42.

60. Muller S, Scaffidi P, Degryse B, Bonaldi T, Ronfani L, Agresti A, et al. The double life of HMGB1 chromatin protein: architectural factor and extracellular signal. Embo J 2001;20:4337-40.

61. Taguchi A, Blood DC, del Toro G, Canet A, Lee DC, Qu W, et al. Blockade of RAGE-amphoterin signalling suppresses tumour growth and metastases. Nature 2000;405:354-60.

62. Travers AA. Priming the nucleosome: a role for HMGB proteins? Embo Rep 2003;4:131-6.

63. Ito T, Kawahara K, Nakamura T, Yamada S, Nakamura T, Abeyama K, et al. High-mobility group box 1 protein promotes development of microvascular thrombosis in rats. J Thromb Haemost 2007;5:109-16.

64. Gardella S, Andrei C, Ferrera D, Lotti LV, Torrisi MR, Bianchi ME, et al. The nuclear protein HMGB1 is secreted by monocytes via a non-classical, vesicle-mediated secretory pathway. Embo Rep 2002;3:995-1001.

65. Bonaldi T, Talamo F, Scaffidi P, Ferrera D, Porto A, Bachi A, et al. Monocytic cells hyperacetylate chromatin protein HMGB1 to redirect it towards secretion. Embo J 2003;22:5551-60.

66. Taguchi A, Blood DC, del Toro G, Lu A, Canet A, Ou W, et al. Blockade of amphoterin-receptor for age (RAGE) interaction suppresses lung metastasis in murine Lewis lung carcinoma. Faseb Journal 1999;13:A363-A.

67. Muller S, Ronfani L, Bianchi ME. Regulated expression and subcellular localization of HMGB1, a chromatin protein with a cytokine function. J Intern Med 2004;255:332-43.

68. Choi YR, Kim H, Kang HJ, Kim NG, Kim JJ, Park KS, et al. Overexpression of high mobility group box 1 in gastrointestinal stromal tumors with *KIT* mutation. Cancer Res 2003;63:2188-93.

69. Volp K, Brezniceanu ML, Bosser S, Brabletz T, Kirchner T, Gottel D, et al. Increased expression of high mobility group box 1 (HMGB1) is associated with an elevated level of the antiapoptotic c-IAP2 protein in human colon carcinomas. Gut 2006;55:234-42.

70. Kang HJ, Koh KH, Yang EG, You KT, Kim HJ, Paik YK, et al. Differentially expressed proteins in gastrointestinal stromal tumors with *KIT* and *PDGFRA* mutations. Proteomics 2006;6:1151-7.

71. Youn JH, Shin JS. Nucleocytoplasmic shuttling of HMGB1 is regulated by phosphorylation that redirects it toward secretion. J Immunol 2006;177:7889-97.

72. Dumitriu IE, Baruah P, Bianchi ME, Manfredi AA, Rovere-Querini P. Requirement of HMGB1 and RAGE for the maturation of human plasmacytoid dendritic cells. Eur J Immunol 2005;35:2184-90.

73. Raucci A, Palumbo R, Bianchi ME. HMGB1: A signal of necrosis. Autoimmunity 2007;40:285-9.

74. Fiuza C, Bustin M, Talwar S, Tropea M, Gerstenberger E, Shelhamer JH, et al. Inflammation-promoting activity of HMGB1 on human microvascular endothelial cells. Blood 2003;101:2652-60.

75. Orlova VV, Choi EY, Xie CP, Chavakis E, Bierhaus A, Ihanus E, et al. A novel pathway of HMGB1-mediated inflammatory cell recruitment that requires Mac-1-integrin. Embo J 2007;26:1129-39.

76. Dumitriu IE, Baruah P, Valentinis B, Voll RE, Herrmann M, Nawroth PP, et al. Release of high mobility group box 1 by dendritic cells controls T cell activation via the receptor for advanced glycation end products. J Immunol 2005;174:7506-15.

77. Scaffidi P, Misteli T, Bianchi ME. Release of chromatin protein HMGB1 by necrotic cells triggers inflammation. Nature 2002;418:191-5.

78. Ito I, Mitsuoka N, Sobajima J, Uesugi H, Ozaki S, Ohya K, et al. Conformational difference in HMGB1 proteins of human neutrophils and lymphocytes revealed by epitope mapping of a monoclonal antibody. J Biochem 2004;136:155-62.

79. Stemmer C, Schwander A, Bauw G, Fojan P, Grasser KD. Protein kinase CK2 differentially phosphorylates maize chromosomal high mobility group B (HMGB) proteins modulating their stability and DNA interactions. J Biol Chem 2002;277:1092-8.

80. Nishizuka Y. Intracellular Signaling by Hydrolysis of Phospholipids and Activation of Protein-Kinase-C. Science 1992;258:607-14.

81. Paolucci L, Rozengurt E. Protein kinase D in small cell lung cancer cells: Rapid activation through protein kinase C. Cancer Res 1999;59:572-7.

82. Burgering BMT, Devriessmits AMM, Medema RH, Vanweeren PC, Tertoolen LGJ, Bos JL. Epidermal Growth-Factor Induces Phosphorylation of Extracellular Signal-Regulated Kinase-2 Via Multiple Pathways. Mol Cell Biol 1993;13:7248-56.

83. Goode N, Hughes K, Woodgett JR, Parker PJ. Differential Regulation of Glycogen-Synthase Kinase-3-Beta by Protein-Kinase-C Isotypes. J Biol Chem 1992;267:16878-82.

84. Hug H, Sarre TF. Protein-Kinase-C Isoenzymes - Divergence in Signal Transduction. Biochem J 1993;291:329-43.

85. Newton AC. Regulation of protein kinase C. Curr Opin Cell Biol 1997;9:161-7.

86. Newton AC. Regulation of protein kinase C's membrane interaction by two membrane-targeting domains? Biophys J 1997;72:Tup88-Tup.

87. Keranen LM, Newton AC. Ca2+ differentially regulates conventional protein kinase Cs' membrane interaction and activation. J Biol Chem 1997;272:25959-67.

88. Cambier JC, Newell MK, Justement LB, Mcguire JC, Leach KL, Chen ZZ. Ia Binding Ligands and Camp Stimulate Nuclear Translocation of Pkc in Lymphocytes-B. Nature 1987;327:629-32.

89. Filomenko R, Poirson-Bichat F, Billerey C, Belon JP, Garrido C, Solary E, et al. Atypical protein kinase C zeta as a target for chemosensitization of tumor cells. Cancer Res 2002;62:1815-21.

90. Malviya AN, Block C. Nuclear-Protein Kinase-C and Signal-Transduction. Receptor 1993;3:257-75.

91. La Porta CAM, Dolfini E, Comolli R. Inhibition of protein kinase C-alpha isoform enhances the P-glycoprotein expression and the survival of LoVo human colon adenocarcinoma cells to doxorubicin exposure. Brit J Cancer 1998;78:1283-7.

92. Lu Y, Jamieson L, Brasier AR, Fields AP. NF-kappa B/RelA transactivation is required for atypical protein kinase C iota-mediated cell survival. Oncogene 2001;20:4777-92.

93. Greif H, Benchaim J, Shimon T, Bechor E, Eldar H, Livneh E. The Protein-Kinase C-Related Pkc-L(Eta) Gene-Product Is Localized in the Cell-Nucleus. Mol Cell Biol 1992;12:1304-11.

ABSTRACT IN KOREAN

위장관 종양에서 Receptor Tyrosine Kinase (*KIT* 및 *PDGFRA*) 유전자 돌연변이 및 HMGB1 활성이 암발생과 진행에 미치는 영향

Hyun Ju Kang

Department of Medical Science

The Graduate School, Yonsei University

(Directed by Professor Hoguen Kim)

위장관간질종양은 위와 장에 발생하는 대표적인 간엽성 종양(mesenchymal tumor)으로 현재까지 수행된 분자유전학적 연구결과에 따르면, 약 41~92%의 위장관간질종양에서 *v-kit Hardy-Zuckerman 4 feline sarcoma viral oncogene homolog (KIT)* 종양형성유전자의 gain-of-function 돌연변이가 있음이 확인되었다. 최근 연구에 따르면 *KIT* 유전자 변이가 없는 위장관간질종양 중 일부에서 동일한 receptor tyrosine kinase III 그룹에 속하는 *platelet-derived growth factor receptor a (PDGFRA)* 유전자의 활성변이가 있음이 관찰되었으며 이러한 두 유전자의 활성변이는 상호배타적으로 일어나는 현상임이 보고되었다. 두 유전자의

변이는 위장관간질종양의 발암과정에서 비슷한 생물학적 결론을 도출해 낼 것으로 예상되고, 실제 주요한 신호전달경로의 활성이 동일하게 일어남이 밝혀졌다. 그러나 이들 유전자의 변이가 위장관간질종양에서 종양 발생 및 진행과정에 미치는 명확한 기전 및 관련 인자에 관한 연구는 아직 부족하다. 뿐만 아니라 위장관간질종양에서 *KIT* 과 *PDGFRA* 변이 상태에 따라 종양세포의 형태나 크기, 분열능 등의 임상병리학적 특징 및 약물치료에 대한 반응도의 차이가 있음이 알려짐에 따라, 각각의 유전자 특이적이 신호전달경로의 규명이 필요하게 되었다.

본 연구에서는 위장관간질종양에서 *KIT* 및 *PDGFRA* 유전자의 변이 및 여러 임상유전학적 특성에 따른 전사체 및 단백의 체계적 검증을 위하여 전체 23 예의 위장관간질종양 환자의 조직을 대상으로 22 예의 조직에서는 microarray 검사를 수행하고, 12 예에서는 이차원적 전기영동 기술을 이용한 프로테옴 분석을 수행하였다. *KIT* 및 *PDGFRA* 유전자 돌연변이 양상에 따라 해당 유전자의 전사체 및 단백질 발현 양이 증가하였고, 각 유전자 돌연변이 양상에 따라 활성화 되는 하부신호 전달기전에 차이가 있음을 확인 할 수 있었다. 또한 돌연변이 양상에 따라 발현 양상의 차이를 보이는 70 개의 전사체 및 15 개의 단백질을 발굴하였다.

이와 함께 위장관간질종양의 진행에 관련된 분자적 기작을 확인하기 위해 악성도에 따라 발현 차이를 보이는 단백질을 분석한 결과 고위험군(high risk)에 속하는 위장관간질종양에서 과발현 양상을 보이는 5 개의

단백질 (Annexin V, HMGB1, C13orf2, Glutamate dehydrogenase 1 과 Fibrinogen beta chain)을 발굴하였다. 이중 모든 위장관간질종양에서 발현되며, non-histone 핵 단백질의 일종으로 전사인자와 상호작용하여 세포의 이동에 관여한다고 알려진 HMGB1 단백질이 초저위험군 (low risk)에 비해 고위험군 (high risk)에서 2.35 배 이상의 과발현 되었다. 특히 정상 대조조직과의 비교를 통해 HMGB1 의 과발현과 세포질에 존재함을 위장관간질종양과 대장암에서 확인하였다. 이러한 암세포 내 HMGB1 단백의 위치 변화는 암 세포주를 통한 벡터 트랜스펙션과 약물처리 실험을 통해 PKC-δ에 의한 HMGB1 의 인산화에 기인된 것 임을 관찰하였고, 인산화된 HMGB1 단백질은 결국 세포 밖에서 검출되었으며, 세포밖에 HMGB1 을 투여한 경우 암세포의 침윤 등이 증가함을 확인하였다.

결론적으로 본 연구는 위장관간질종양에서 유전자 발현 패턴과 단백질체 발현을 분석함으로써 유전자 변이와 임상병리학적 특성에 따라 구분되는지는 요소를 확인하였다. 이 중 변이 상태에 따라 발현이 의미 있게 변화한 유전자들을 동정하고, 활성화된 단백질 패턴을 분석함으로써 유전자 특이적인 신호체계를 확인함으로써 이들 유전자가 암 진행에 미치는 영향 및 기능을 일부 확인하였다. 또한 암조직에서 과발현 하는 핵단백질인 HMGB1 은 PKC 경로로 인산화되어 핵에서 유리되어 세포질로 이동하고, 궁극적으로는 세포외부로 배출되어 암세포의 침윤과 이동을 증가시키는 인자로 작용함을 밝혔다. 이러한 연구결과는 *KIT* 과 *PDGFRA*

유전자의 작용 기작 및 RTK 의 신호전달경로를 밝혀냄으로써, 위장관간질종양 뿐만 아니라 다른 암에서의 임상적, 병리학적, 분자생물학적 특징에 따른 특화된 암 치료법 개발에 기여하리라 사료된다.

핵심 되는 말: 위장관 간질 종양, KIT, PDGFRA, 유전자 발현 프로파일링, 올리고 마이크로어래이, 프로테오믹스, HMGB1

PUBLICATION LIST

1. Choi YR, Kim H, Kang HJ, Kim NG, Kim JJ, Park KS, et al. Overexpression of high mobility group box 1 in gastrointestinal stromal tumors with *KIT* mutation. Cancer Res. 2003;1:63(9):2188-93.

2. Kang HJ, Nam SW, Kim H, Rhee H, Kim NG, Kim H, et al. Correlation of *KIT* and *platelet-derived growth factor receptor alpha* mutations with gene activation and expression profiles in gastrointestinal stromal tumors. Oncogene. 2005;3:24(6):1066-74.

3. Kang HJ, Koh KH, Yang E, You KT, Kim HJ, Paik YK, et al. Differentially expressed proteins in gastrointestinal stromal tumors with *KIT* and *PDGFRA* mutations. Proteomics. 2006;6(4):1151-7.